

A MATHEMATICAL MODEL OF STEADY STATE

B LYMPHOPOIESIS IN MOUSE AND RAT BONE MARROW

Özge Karanfil

Department of Physiology
McGill University
Montreal, Quebec, Canada

October 2007

A thesis submitted to the Faculty of Graduate Studies and Research
in partial fulfillment of the requirements for the degree of Master of Science

© Özge Karanfil 2007



Library and
Archives Canada

Published Heritage
Branch

395 Wellington Street
Ottawa ON K1A 0N4
Canada

Bibliothèque et
Archives Canada

Direction du
Patrimoine de l'édition

395, rue Wellington
Ottawa ON K1A 0N4
Canada

Your file Votre référence
ISBN: 978-0-494-38405-3
Our file Notre référence
ISBN: 978-0-494-38405-3

NOTICE:

The author has granted a non-exclusive license allowing Library and Archives Canada to reproduce, publish, archive, preserve, conserve, communicate to the public by telecommunication or on the Internet, loan, distribute and sell theses worldwide, for commercial or non-commercial purposes, in microform, paper, electronic and/or any other formats.

The author retains copyright ownership and moral rights in this thesis. Neither the thesis nor substantial extracts from it may be printed or otherwise reproduced without the author's permission.

AVIS:

L'auteur a accordé une licence non exclusive permettant à la Bibliothèque et Archives Canada de reproduire, publier, archiver, sauvegarder, conserver, transmettre au public par télécommunication ou par l'Internet, prêter, distribuer et vendre des thèses partout dans le monde, à des fins commerciales ou autres, sur support microforme, papier, électronique et/ou autres formats.

L'auteur conserve la propriété du droit d'auteur et des droits moraux qui protègent cette thèse. Ni la thèse ni des extraits substantiels de celle-ci ne doivent être imprimés ou autrement reproduits sans son autorisation.

In compliance with the Canadian Privacy Act some supporting forms may have been removed from this thesis.

While these forms may be included in the document page count, their removal does not represent any loss of content from the thesis.

Conformément à la loi canadienne sur la protection de la vie privée, quelques formulaires secondaires ont été enlevés de cette thèse.

Bien que ces formulaires aient inclus dans la pagination, il n'y aura aucun contenu manquant.


Canada

ACKNOWLEDGMENTS

I would like to express my deepest gratitude to Prof. Michael C. Mackey, my thesis supervisor, for his invaluable guidance and support throughout all phases of this research, and for his patience.

I would like to express my deepest gratitude to Prof. Dr. Dennis Osmond, for providing his group's laboratory data of lifelong study, for the many fruitful discussions that we had together to discuss several aspects of B lymphopoiesis meticulously, and for showing me a great hospitality in Ottawa.

I would like to thank Prof. Michael Guevara, Prof. Kathleen E. Cullen, and Prof. Leon Glass for taking part in my thesis committee and providing valuable comments about this research.

I wish to express my deepest gratitude to my parents, Gül and Hüseyin Karanfil and to my sister Simge Karanfil, for their never ending support and affection.

I finally wish to thank all of my friends for being with me in my last two years in Montreal. I am also thankful to the members of Center for Nonlinear Dynamics for their understanding and support during my study.

ABSTRACT

In this study, we have analyzed the steady-state kinetics of B lymphocytes in mouse and rat bone marrow using previously published experimental data. Over many years, Prof D.G. Osmond and his colleagues have built up a scheme of B cell development in mouse bone marrow based on the sequential expression of markers associated with the B lineage. The earliest precursor B cells comprise three populations of proliferating pro-B cells, i.e. early, intermediate, and late pro-B cells. The subsequent populations comprise pre-B cells that give rise to nondividing B lymphocytes expressing surface IgM.

In our analysis, we have checked the available published data for consistency with the proliferation of precursor B cells and their death via apoptosis at certain stages of cell development. We made an extensive summary of the existing data on the various B cell precursors and organized it into a comprehensible framework. We built a mathematical model for the proliferation and differentiation of mammalian B lymphocytes in laboratory mice and rats and estimated all of the parameters to explain the existing steady state data. In this context, mathematical modeling acts as a useful tool to analyze hypotheses and experimental results concerning the steady state numbers of B lymphocytes.

RESUME

Dans cette étude, nous avons analysé la cinétique de l'état stationnaire de lymphocytes B provenant de la moelle osseuse de souris et de rat en utilisant des données expérimentales publiées précédemment. Précédemment, le professeur D.G. Osmond et ses collègues ont élaboré un schéma de développement des lymphocytes B en provenance de moelle osseuse de souris sur la base de l'expression séquentielle d'un marqueur associé à la lignée de lymphocytes B. Les plus récentes cellules B précurseurs comprennent trois populations de cellules pré-B qui ont permis l'éclosion de lymphocytes B non proliférantes exprimant la protéine IgM membranaire.

Dans notre analyse, nous avons vérifié la cohérence des données disponibles avec la prolifération des cellules B précurseurs et leur mort par apoptose à certains stades du développement des cellules. Nous avons fait un sommaire complet des données existantes pour diverses cellules B précurseurs et les avons organisées à l'aide d'un cadre de référence intelligible. Nous avons construit un modèle mathématique de la prolifération et de la différenciation des lymphocytes B (mammifères) des souris et rats et estimé tous les paramètres expliquant les données actuelles de l'état stationnaire. Dans ce contexte, la modélisation mathématique est utile pour analyser les hypothèses et les résultats expérimentaux concernant le nombre de lymphocytes B à l'état stable.

TABLE OF CONTENTS

ACKNOWLEDGMENTS	ii
ABSTRACT.....	iii
RESUME	iv
LIST OF FIGURES	vi
LIST OF TABLES.....	viii
LIST OF ABBREVIATIONS.....	x
1. INTRODUCTION	1
2. SURVEY OF LYMPHOCYTE PHYSIOLOGY AND PRODUCTION	2
2.1. Lymphocyte Production in Bone Marrow	2
2.2. Apoptosis in Bone Marrow	2
2.3. Mathematical and Conceptual Models.....	4
2.3.1. Methods/Techniques Employed.....	4
2.3.2. Mathematical and Conceptual Models of Lymphocytes.....	6
3. THE DATA.....	10
3.1. Mice Data- Osmond Scheme	10
3.1.1. Kinetics of B cell Production in Mouse Bone Marrow.....	12
3.1.2. Kinetics of B cell Apoptosis in Mouse Bone Marrow.....	22
3.2. Rat Data- Opstelten Scheme	29
3.2.1. Kinetics of B cell Production in Rat Bone Marrow	30
4. PROBLEM DESCRIPTION AND RESEARCH OBJECTIVE.....	36
5. DESCRIPTION OF MODEL	39
5.1. Summary of Parameters and Flows for Mice.....	41
5.2. Summary of Parameters and Flows for Rat	43
6. ANALYSIS OF THE MODEL.....	46
6.1. Relevancy of the Late Pro-B cells.....	46
6.2. Reflux due to Receptor Editing.....	49
7. CONCLUSION AND FUTURE WORK	51
GLOSSARY	54
REFERENCES	55

LIST OF FIGURES

Figure 3.1: Phenotypic scheme of B-cell development in mouse BM (from Osmond, 2000)	11
Figure 3.2: I_{met} of pre-B cells after vincristine. The curves were obtained by linear regression analysis of the 12 values for the I_{met} in vincristine-injected mice. The data are derived from three separate experiments (from Opstelten and Osmond, 1983).....	17
Figure 3.3: I_{met} of pre-B cells (Data from Opstelten and Osmond, 1983- Figure 4,)...	18
Figure 3.4: Disappearance of cells unlabeled by ^3H -thymidine from the BM of all small lymphocytes (\times), non-Ag-binding small lymphocytes (\bullet) and small lymphocytes binding antiglobulin- ^{131}I in a concentration of 1.0 $\mu\text{g/ml}$ (\blacksquare , by observation; \square , by calculation) during repeated administration of ^3H -thymidine <i>in vivo</i> (from Osmond and Nossal, 1974)	20
Figure 3.5: Disappearance of unlabeled cells, and the fitted exponential functions for	21
Figure 3.6: Incidence of hypodiploid cells at various phenotypic stages of B cell development in freshly prepared BM cell suspensions detected by flow cytometry. <i>A</i> , Incidence of apoptotic B cells within each defined compartment. <i>B</i> , Frequency of apoptotic B cells per 1000 total nucleated BM cells. Data were derived from four separate experiments (mean \pm SD) (from Lu and Osmond, 1997).....	23
Figure 3.7: Incidence of hypodiploid cells, detected by flow cytometry in mouse BM suspensions during 0- to 8-h incubation.	25
Figure 3.8: Incidence of hypodiploid cells detected by flow cytometry in mouse BM suspensions during 0- to 8-h incubation (given in hours) with or without a	

monolayer of stromal cells. Data represent three separate experiments
(mean \pm SD) (*from Lu and Osmond, 1997*). 26

Figure 3.9: I_{met} of HIS24+ BM cell subsets after vincristine. The lines were obtained by linear regression analysis of 15 ($\text{cu}^+\text{s}\mu^-$, HIS24 $^+$ TdT $^-\mu^-$) or 16 (TdT $^+$) values for I_{met} in vincristine-injected rats (*from Deenen, Hunt and Opstelten, 1987*)..... 33

Figure 3.10: Disappearance of cells unlabeled (BrdUrd-) sIgM+ B lymphocytes and small B precursor cells in rat BM during continuous infusion of BrdUrd.
(a) sIgM+ B lymphocytes; (b) small (<11 μm) pre-B cells; (c) small (<12 μm) TdT+ cells; (d) small (<11 μm) HIS24+TdT-Ig- cells (*from Deenen, Balen and Opstelten, 1990*)..... 35

Figure 5.1: Flows for a hypothetical compartment of size N 40

Figure 6.1: Testing the hypothesis of “reflux” from immature B cell to small pre-B cell pool- Change in model structure 49

LIST OF TABLES

Table 3.1: Cell markers of the phenotypically defined B cell compartments in Mouse BM	12
Table 3.2: Kinetic state of the phenotypically defined B cell compartments in Mouse BM	12
Table 3.3: Parameter values for the B cell size in Mouse BM	13
Table 3.4: Parameter values for the population size of B cells in Mouse BM.....	14
Table 3.5: Parameter values for the kinetics of B cell proliferation in Mouse BM.....	18
Table 3.6: Parameter values for the kinetics of B cell turnover in Mouse BM	22
Table 3.7: Summary of the parameter values for the kinetics of B cell production and turnover in BM.....	27
Table 3.8: Summary of the parameter values for the kinetics of B cell apoptosis in BM	28
Table 3.9: Cell markers of the phenotypically defined B cell compartments in Rat BM	30
Table 3.10: Kinetic state of the phenotypically defined B cell compartments in Rat BM	30
Table 3.11: Parameter values for the cell size in Rat BM.....	31
Table 3.12: Parameter values for the population size of B cells in Rat BM.....	32
Table 3.13: Parameter values for the kinetics of B cell proliferation in Rat BM	34

Table 3.14: Parameter values for the kinetics of B cell turnover in Rat BM.....	35
Table 5.1: Summary of flows between compartments and number of mitoses-for Mouse.....	42
Table 6.1: Steady state flows when late pro-B cells are reduced by 25%	47
Table 6.2: Time constants when late pro-B cells are reduced by 25%	47
Table 6.3: Steady state flows when late pro-B cells are reduced by 50%	47
Table 6.4: Time constants when late pro-B cells are reduced by 50%	48
Table 6.5: Steady state flows when late pro-B cells are reduced by 100%	48
Table 6.6: Time constants when late pro-B cells are reduced by 100%	48
Table 6.7: Steady state flows after imposing a “reflux” of 0.2% from immature B cell to small pre-B cell pool.....	49

LIST OF ABBREVIATIONS

B220	B lineage surface membrane B220 glycoprotein (CD45RA isoform)
BCR	B Cell Receptor
BM	Bone Marrow
BrdU	Bromodeoxyuridine (or BrdUrd)
CFSE	CarboxyFluorescein diacetate Succinimidyl Ester
CFU	Colony forming unit
CFU-S	Very primitive hemopoietic precursors
CSF	Colony-stimulating factor
Dex	Dexamethasone
Go	Non-cycling or resting phase of the cell cycle
G1	Pre-DNA synthetic phase (or post-mitotic) of the cell cycle
HIS24	B lineage surface antigen expressed in rat bone marrow B cells
HSC	Haematopoietic stem cells
³ H-TdR	Tritiated thymidine
I _{met}	Metaphase incidence (%), M phase index, or the rate of the increase in the percentage of cells in metaphase
I _s	Incidence of DNA synthesis or S phase index
I _{apop}	Apoptotic incidence (or index)
IL	Interleukin
M _i	The number of mitotic cycles within compartment <i>i</i>
M	Mitosis phase of the cell cycle
S	DNA synthetic phase of the cell cycle
SRBC	Sheep red blood cells
TdT	(Intranuclear) Terminal deoxynucleotidyl transferase
cμ	Intracytoplasmic μ chains
r _M	Rate of entry into mitosis
scid	Severe combined immunodeficiency
sIgM	Surface immunoglobulin M, stable surface IgM
sIdD	Surface immunoglobulin D
sμ	Surface μ chains

$t_{c(a)}$	Apparent average cell cycle time
t_S	Average duration of DNA sythesis
t_M	Average duration of mitosis
$t_{1/2}$	The time for fifty percent turnover
τ_i	Average length of time that cells spend in compartment i
β_i	Proliferation rate constant in compartment i
γ_i	Apoptotic rate constant in compartment i
δ_i	Output rate constant in compartment i
Φ	Total number of nucleated cells per femur
\sum_i^i	Sum of inflows in compartment i
\sum_i^o	Sum of outflows in compartment i

1. INTRODUCTION

Unlike the parallel processes of erythropoiesis and granulopoiesis, the regulation of the subpopulations of progenitors and non-dividing progeny in bone marrow (BM) lymphopoiesis is less well quantified. Moreover, the use of dissimilar phenotypic criteria in different laboratories has led to the formulation of disparate models of lymphopoiesis that are not fully consistent with each other.

In this study, we have analyzed the steady-state kinetics of B lymphocytes in bone marrow using previously published experimental data from mouse and rat B cells. Over many years, Prof D.G. Osmond and his colleagues have built up a scheme of B cell development in mouse bone marrow based on the sequential expression of three markers associated with the B lineage: 1) surface membrane B220 glycoprotein, 2) intranuclear terminal deoxynucleotidyl transferase (TdT), and 3) μ heavy chains of IgM expressed in the cytoplasm (c μ) or at the cell surface (s μ) in the B cell antigen receptor. The earliest precursor B cells comprise three populations of proliferating pro-B cells, i.e. early, intermediate, and late pro-B cells. The subsequent B 220⁺ populations comprise pre-B cells that give rise to nondividing B lymphocytes expressing surface IgM.

In our analysis, we have checked the published data for consistency with the proliferation of precursor B cells and their death via apoptosis at certain stages of cell development. We were able to make an extensive summary of the existing data on the various B cell precursors and to organize it into a comprehensible framework. We built a mathematical model for the proliferation and differentiation of mammalian B lymphocytes in laboratory mice and rats and estimated all of the parameters to explain the existing steady state data (e.g. the calculated flow from 'compartment' to 'compartment', the number of mitoses, and number of cells per clone).

2. SURVEY OF LYMPHOCYTE PHYSIOLOGY AND PRODUCTION

2.1. Lymphocyte Production in Bone Marrow

Approximately a quarter of all nucleated cells in the BM of laboratory mammals, the human foetus and infant may be classified as lymphoid cells (Osmond *et al.*, 1983). They are heterogeneous with respect to many properties: their morphology, cell size, chromatin condensation, functions, etc., and their definition and kinetic properties is less well understood than in erythrocytes and granulocytes. However as with every other cell lineage, production of lymphocytes represents a balance between the proliferation of its precursor cells, and their death at some critical stages of cell development. These processes depend on microenvironmental signals, but also respond to systemic factors (Lu and Osmond, 2001). However, the homeostatic mechanisms that control the lymphocyte production also remain poorly understood.

The production and kinetics of BM lymphocytes is studied extensively in mice, guinea pig, and rat. In these species the BM contains a large number of newly formed small lymphocytes, which can be distinguished by their minimal quantity of cytoplasm and a spherical or slightly intended nucleus. These “immature B cells” are then exported from the BM to the periphery as “transitional” cells, and they are subject to further selection. The surviving transitional cells complete their maturation and join the mature naive peripheral B cell pool (Mehr *et al.*, 2003)

2.2. Apoptosis in Bone Marrow

For many years, lymphopoiesis research has been focused only on cell production and its regulation in mammalian BM. However more recently, macrophage mediated deletion of lymphocytes has been recognized *in vivo*, and apoptosis appeared

as an important regulatory process which contributes to the homeostasis of cell populations (Osmond *et al.*, 1994). At the same time, increasing numbers of molecular markers and the use of genetically modified mice have opened up new possibilities for research, and attention has reverted to the problem of cell loss.

Normally, cells are known to have biological programs for suicide, as well as for replication. Apoptosis (programmed cell death) is one of the pathways for cell death, the other one being necrosis (accidental cell death) (See the website http://sciencepark.mdanderson.org/fcores/flow/files/DNA_PI.html). Apoptosis differs from necrosis by self initiation, and includes events such as “an early surface expression of phosphatidylserine that is normally confined to the inner aspect of the plasma membrane, chromatin condensation, nucleosomal DNA fragmentation, and hypodiploid DNA content” (Lu and Osmond, 1997), which is followed by phagocyte ingestion.

It is known that B lineage cells in BM undergo apoptosis at a higher rate than non-B lineage cells in BM (Lu and Osmond, 1997). The physiological significance of this extensive cell deletion may be to maintain lymphocyte homeostasis by determining the magnitude of the final output to the peripheral immune system, and to check the quality of the renewing cell populations of the body (Osmond *et al.*, 1994).

Apoptosis is influenced by local microenvironmental signals in the BM, but also responds to systemic circulatory factors. However, factors that may regulate cell deletion are less well understood than the proliferative factors that regulate lymphocyte production in BM (Lu and Osmond, 2000). Moreover, estimation of cell death rates is more difficult than estimation of cell proliferation and turnover rates, since dead cells are rapidly recognized and cleared from the BM (Mehr *et al.*, 2003). The number of apoptotic cells that can be measured at any given time is small, and this measure (incidence of apoptosis, or apoptotic index) alone cannot provide sufficient information to predict the actual magnitude of apoptosis within any cell population *in vivo* (Lu and Osmond, 1997, 2000). Thus, the rate of entry into

apoptosis is a more direct measurement of the extent of programmed cell death than the apoptotic index (Lu and Osmond, 2000).

2.3. Mathematical and Conceptual Models

2.3.1. Methods/Techniques Employed

As mentioned above, several aspects of lymphocyte have been identified by different laboratories using different phenotypic criteria and terminology, and a variety of techniques. Since mathematical analyses are based on the data sets provided by these laboratories, the use of different techniques also poses some limitations and/or advantages for related mathematical models. Moreover, there is controversy about the techniques used and their reliability, since they have led to conflicting results in the past. This offers a strong cautionary note that the raw data provided by the laboratory should be carefully interpreted by modelers by taking the limitations of the collected data and the method of collection into account, since data can be mistakenly interpreted in the absence of an underlying theory.

Earlier approaches benefited from the use of labeled DNA precursors, which appeared as an obvious method to study the cell cycle, DNA synthesis and cellular proliferation (Bonhoeffer *et al.*, 2000). These biological markers were incorporated into the DNA of the cell and then shared between their daughter cells on division. ^3H -TdR (tritiated thymidine) is one of these markers that were extensively used after World War II to study cell division *in vivo* and *in vitro* (Bernard *et al.*, 2003). Takahashi (1966) and Lebowitz and Rubinow (1969) carried out mathematical models of ^3H -TdR data.

However, ^3H -TdR is a radiolabeled precursor which can induce apoptosis (Yanokur, 2000) and significantly perturb the experimental conditions. So it has later been replaced by safer nonradioactive molecules, such as the base analog 5-Brom-2-deoxyuridine (BrdU or BrdUrd) (Bonhoeffer, 2000). Cells labeled with BrdU can be

detected by immunofluorescence or via flow cytometry. This method has been used extensively as a reliable procedure to study division, life span, and turnover of cell populations of both B and T lymphocytes (Forster and Rajewski 1990, Thoug and Sprent 1994, 1998, Rocha *et al.* 1990, Forster, 2004), and related mathematical analyses are carried out by Bertuzzi *et al.* (2002), Forster *et al.* (1989), Gratzner (1982), Houck and Loken (1985) and Bonhoeffer *et al.* (2000). The logic of “continuous” labeling by using BrdU to measure the turnover of cell populations is explained in Section 2.1.

The main problem with using labeled DNA precursors like ^3H -TdR or BrdU is that they cannot give the division history of individual cells, i.e. they are unable to track the number of divisions that a cell has undergone (Bernard *et al.*, 2003). (I will correct this paragraph, Dr. Mackey said that this is not true, and there is a method called silver “grain count” labeling which uses thymidine and is able to track the division history of cell) More recently, this problem is also solved by using a new tracking dye, the Carboxyfluorescein diacetate Succinimidyl Ester (CFSE). CFSE is an intracellular fluorescent label for lymphocytes which labels both resting and proliferating cells and divides equally between daughter cells during cell division both *in vitro* and *in vivo* (Hodgkin *et al.*, 1996; Lyons and Parish, 1994). It is currently the most accurate labeling technique to study the division history of cells. Moreover, changes in cell phenotype are unaffected by CFSE labeling. Gett and Hodgkin (2000) pioneered the first mathematical analyses using CFSE data, and their approach is recently extended by De Boer *et al.* (2006). A typical CFSE dataset includes both the number of cells $X(t)$ as well as the CFSE division profile at given time points following CFSE labeling (workshop paper). The main limitation of this approach is that fluorescence can only be detected up to seven or eight cell divisions, since the label dilutes 2-fold on each cell division: After 8 divisions the CFSE intensity is 2^8 fold lower than its original intensity. (Oostendorp *et al.*, 2000).

2.3.2. Mathematical and Conceptual Models of Lymphocytes

2.3.2.1. B Lymphocytes: Most of the existing mathematical analyses of B cells model only B cell populations in the periphery (cells outside of the BM), and the emphasis is on homeostatic regulation, and competition for resources.

McLean *et al.* (1997) developed a mathematical model of the peripheral regulation of B cell numbers. This study investigates the role of competition for resources by using a Lotka-Volterra type of competition model with the addition of immigration. Accordingly, the size of the peripheral B cell pool is mainly affected by: 1) immigration from the BM; 2) competition for resources in periphery; and 3) death of cells which cannot secure resources. All BM precursor cells are modeled as one group, and their growth is described by a logistic equation. Both BM and peripheral B cell numbers are limited by corresponding carrying capacities, and the peripheral B cell growth rate is also defined as a nonlinear relationship of population size. Two different types of competition are presented and data on B lymphocyte populations (Freitas *et al.*, 1995) are compared to the first model. Model results imply that out of a population of 50 million splenic B cells at steady state, 5 million are supported by resources, and the rest of 45 million cells are regulated by immigration and death, in which death rates are modulated by competition.

DeBoer *et al.* (2001) employed a similar approach to investigate competition among B cells, which allows for various B cell clones, generated in the BM, to migrate to the periphery and compete specifically for various ligands (resources). Model results demonstrate that most of the variation in the data can be explained by “intraspecific competition” within the clones, rather than “inter-specific” competition between repertoires.

Recently, Mehr *et al.* (2003) presented the first quantitative model of the population dynamics of precursor B cells in the mouse BM using BrdU labeling data. The scheme used in the model is comprised of five precursor compartments, i.e. the pro-B, pre-B and immature B cells, of which the pro- and pre-B cells are divided into

cycling and resting compartments. It is suggested that B cell development may not be completely unidirectional, and a phenotypic reflux may exist between the pre-B and immature B cell pools, possibly caused by receptor editing. Similar to the previous models of B and T cells, a logistic growth limiting factor is imposed on the proliferation of developing B cells, and carrying capacities are defined for each of the five precursor compartments. Cell death is also assumed to occur, but only in the proliferating compartments. Ranges are defined for each parameter that gives results within the experimental range, and then these ranges are narrowed by imposing constraints on parameters, and a data set is found which gives the best fit to experimental results.

Shahaf *et al.* (2004) used mathematical modeling to simulate splenic B cell population dynamics, and determined which of the alternative differentiation models for transitional B cell maturation fits best to the existing labeling data. All the alternatives of transitions between subsets are defined for splenic B cells (a total of 630 alternatives) and then best fits are chosen. Modeling results indicate that best fit is achieved when some cells skip and pass directly into the later stages, and it is suggested that B lineage differentiation is an asynchronous and branched process, rather than unidirectional.

A good review of the “conceptual” models for peripheral B cell development and homeostasis is provided by Srivastava *et al.* (2005), which summarizes and compares all the classification criteria of peripheral B cells by different groups, and related concepts and hypotheses.

The work of Prof. Landreth and his coworkers provides a basic understanding for B cell lineage and its regulatory influences in the BM. Landreth *et al.* identified and segregated B lineage cells into compartments based on the cells' size and expression of the μ heavy chain of IgM (Landreth *et al.*, 1981). They provided a hypothetical scheme for mammalian B cell differentiation, from the haemopoietic stem cell to the newly formed B cell (Landreth *et al.*, 1984). They also addressed regulatory influences on the generation of pre-B cells, and described a situation where

pre-B cell development is dysregulated in association with human cyclic neutropenia, resulting in excessive accumulation of marrow pre-B cells.

Finally, Prof. Osmond and his coworkers also obtained experimental data over a number of years. They developed a scheme of B cell differentiation in the mouse BM which is based on the expression of TdT, B220 cell surface glycoprotein, and μ chains. Their classification system is different than that of Landreth et al; our study is based on Osmond's classification system and experimental data.

2.3.2.2. T Lymphocytes: Ramit Mehr and his colleagues developed a series of mathematical models to illustrate different aspects of T cell development in the mouse thymus. Mehr *et al.* (1997) proposed that T lymphopoiesis (thymocytopoiesis) is subject to feedback regulation by mature lymphocytes, and analysis of the T cell data from *in vitro* experiments is presented using mathematical models. Thymic populations are modeled by first order ODE's, and it is assumed that total number of thymocytes is autonomously controlled, and the competition is expressed in a logistic form with a finite carrying capacity.

Mehr *et al.* (1993) uses the same approach to model the effect of aging on BM cells colonizing the thymus by assuming that the cell cycle duration is the only difference between young and old BM-derived cells. Mehr *et al.* (1995) gives a more detailed analysis for the development of T cells using a four-population model; and specifically for positive and negative selection and differentiation processes in the thymus. Finally, Mehr *et al.* (1996) further develop the previous models to explain the effects of mature T cells present in the thymus on T cell proliferation and differentiation. They suggest that both positive and negative feedback effects are exerted on previous cell populations and possible combinations of feedback are explored.

These articles do not invent new mathematical approaches to examine collected data, but explore and test possible hypothesis and pathways of T cell development and differentiation (such as thymic selection and feedback regulation) by

making use of mathematical modeling and simulation. More recently, Bonhoeffer *et al.* (2000) developed a theory to interpret BrdU measurements, and they illustrated this for the BrdU labeling of T lymphocytes of uninfected and SIV (simian immunodeficiency virus) infected macaques. Analytical expressions are derived for the fraction of labeled cells within growing, declining, and steady-state cell populations. These are then fitted to T cell data to find estimates for the rates of cell proliferation, cell loss, and the rate of cell input from a source.

Gett and Hodgkin (2000) pioneered the use of CFSE data. De Boer *et al.* (2006) extended the method of Gett and Hodgkin by using CFSE data on T lymphocytes to estimate parameters such as the time to first division, the cell cycle time, and the average death rate. Their main assumption was that the T cell death rate depends on the number of divisions a cell has completed. They also fitted the data with a mathematical model derived by reformulating the numerical model of Deenick *et al.* (2003) which is a stochastic model of T cell proliferation.

3. THE DATA

3.1. Mice Data- Osmond Scheme

The use of different phenotypic criteria in different laboratories has led to different formulations of B cell lymphopoiesis, not fully consistent with each other. Additionally, studies which attempt to quantify the populations of B cells in mouse BM also give variable results due to differences between mouse strains, the use of different markers, variability in experimental conditions, and/or differences in methods.

In this study, we will use a scheme which is developed over a number of years by Prof. Osmond and his coworkers. Using immunofluorescence labeling and cell cycle arrest techniques, the Osmond group characterized a B cell differentiation sequence in the mouse BM, which is based on the expression of particular molecules with time:

- 1) Terminal deoxynucleotidyl transferase (**TdT**), expressed in the cell nucleus during immunoglobulin heavy (Ig H) chain gene rearrangement
- 2) **B220** cell surface glycoprotein (not exclusively associated with the B lineage)
- 3) μ chains in cytoplasm (**c μ**), and
- 4) μ chains in IgM molecules expressed at cell surface (**s μ** , **sIgM**)

These four markers define successive stages in B cell development. The earliest defined precursor B cells are called pro-B cells, which is comprised of three populations of proliferating cells before the expression of μ heavy chains. The subsequent B220⁺ populations comprise c μ ⁺ pre-B cells, which give rise to nondividing B lymphocytes expressing surface IgM. These stages are assumed to form a series of concatenated compartments, the 'outflow' from one compartment being the 'inflow' to the next compartment (See Figure 3.1).

- 1) Pro-B cells: Early ($\text{TdT}^+ \text{B220}^-$),
Intermediate ($\text{TdT}^+ \text{B220}^+$),
Late pro-B cells ($\text{TdT}^+ \text{B220}^+$)
- 2) Pre-B cells: $\text{c}\mu^+$ Large
 $\text{c}\mu^+$ Small
- 3) B cells: sIgM^+

Figure 3.1 illustrates the sequence of markers and proliferative status during B lymphopoiesis:

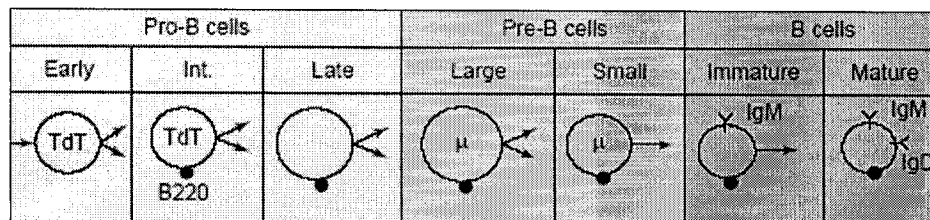


Figure 3.1: Phenotypic scheme of B-cell development in mouse BM (from Osmond, 2000)

3.1.1. Kinetics of B cell Production in Mouse Bone Marrow

3.1.1.1. Age and Strain: To minimize variations in collected data as much as possible, this analysis has been restricted to data sets which belong to the CH HeJ, C57BI/6 and CB/AH Wehi strains of mice, at the age of 10-12 weeks. This is the age of the average adult mice, so the BM cell populations can be assumed to have reached their steady state levels.

3.1.1.2. Cell Markers: The table 3.1 summarizes the cell markers associated with the B lineage, and correlates them with the related stages of B cell development:

Table 3.1: Cell markers of the phenotypically defined B cell compartments in Mouse BM

CELL MARKERS	Pro-B cells			Pre-B cells		B cells
	Early	Int.	Late	Large	Small	
TdT	xxxxxx	xxxxxx				
B220		xxxxxx	xxxxxx	xxxxxx	xxxxxx	xxxxxx
Cytoplasmic μ chains (c μ)				xxxxxx	xxxxxx	
Surface IgM (sIgM)						xxxxxx

3.1.1.3. Kinetic State: The kinetic state of the precursor B compartments is summarized in Table 3.2. Accordingly, all the pro-B cells, and the large pre-B cells are in cell cycle (G_1 , S, G_2 , or M), and the small pre-B cells and the immature B cells are not in cycle (in G_0).

Table 3.2: Kinetic state of the phenotypically defined B cell compartments in Mouse BM

KINETIC STATE	Pro-B cells			Pre-B cells		B cells
	Early	Int.	Late	Large	Small	
Dividing (in cell cycle)	xxxxxx	xxxxxx	xxxxxx	xxxxxx		
Nondividing (in G_0)					xxxxxx	xxxxxx

3.1.1.4. Cell size: The average cell size (cell diameters measured in cytospot preparations), and range of the phenotypically defined precursor B cells are listed in Table 3.3. In our analysis, the cell size data is not used, but from the table it can be

seen that there is a continuum of the modal cell diameters starting from the early pro-B cells to the immature B cells. This supports the premise of the Osmond scheme which states that the defined 'stages' of development form a series of concatenated cell compartments.

Table 3.3: Parameter values for the B cell size in Mouse BM

	Pro-B cells			Pre-B cells		B cells
AVG. CELL SIZE	Early	Int.	Late	Large	Small	
range (μm)		7-13		10-14	7-10	
cell size (μm)	9.0	10.0	12.0	12.0	8.0	8.0

Pro-B cells are medium sized cells measuring 7 to 13 μm in diameter. Intermediate pro-B cells tend to be larger than the early pro-B cells (modal cell diameters of 10 μm and 9 μm) and they progressively increase in size as they mature (Park and Osmond, 1987, 1989; Fulop *et al.*, 1983). Similarly, pre-B cells measure 7 to 13 μm in diameter (modal diameter being 11.5 μm), but they range widely in size. 95% of cells in the large pre-B are larger than 10 μm in diameter, whereas 96% of cells in the small pre-B are less than 10 μm (Lu and Osmond, 1997). This is reasonable since large cycling $\text{c}\mu^+\text{s}\mu^-$ pre-B cells become non-cycling (but rapidly renewing) small pre-B cells. This also suggests that for this particular stage, the compartment boundary between the large pre-B and the small pre-B cells is defined by mitosis.

It is also known that the incidence of metaphase (I_{met}) values of cells increases with cell diameter, which suggests that larger lymphoid cells are more rapidly proliferating than the smaller ones, and have a shorter mean cycle. The modal diameter of $\text{s}\mu^+$ B cells is 8 μm . However a small proportion of $\text{s}\mu^+$ B cells (13%) were larger cells (10-13 μm in diameter), but they were less dense in their $\text{s}\mu$, and those cells were excluded from this study.

3.1.1.5. Population Size: The population size of the precursor B cells in the BM is determined by obtaining different subsets with flow cytometry and multiplying by the total cell count, which gives the total number of cells per femur for a given phenotypically defined compartment. This value can be converted by the estimated

ratio of the total number of cells in the BM to the number in one femur. There is a single estimate for this ratio (15.8), which likely varies between individual mice and between different mouse strains, but nevertheless is used in all calculations in this study to give an estimate for the whole body size of each cell population.

All the parameter values related to the population size are tabulated in Table 3.4. In the first two rows; the incidences are given in terms of the percentage of total nucleated cells, and of B lineage cells in the BM. The number of cells per femur is then calculated by multiplying the incidence (% of total nucleated cells) with the total BM cellularity. Since there are many independent studies with estimations of population size, the mean of the available estimations are used in this table, or the best one is chosen according to the mice strain and age. Accordingly, the estimate for the total nucleated cells per femur (Φ) is given as 161.1×10^5 (Yu *et al.*, 2000). The values for the table are taken from (Opstelten and Osmond, 1983; Miller and Osmond, 1975, Nossal and Osmond, 1974; Par and Osmond, 1987, 1989; Lu *et al.*, 1998).

Table 3.4: Parameter values for the population size of B cells in Mouse BM

POPULATION SIZE	Pro-B cells			Pre-B cells		B cells	Total
	Early	Int.	Late	Large	Small		
Incidence (% of tot. nucleated cells) in BM	0.7	0.9	4.3	3.7	12.4	14.4	36.5
	6.0			16.1			
Incidence (% of B lineage cells) in BM	2.0	2.4	11.9	10.2	34.0	39.5	100.0
	16.3			44.2			
Relative incidence in the group (%)	12.5	14.6	72.9	23.1	76.9	100.0	
	100.0			100.0			
Number of cells per femur ($\times 10^5$): N_f	1.2	1.4	7.0	6.0	20.0	23.2	58.8
Number of cells per whole body BM ($\times 10^6$)	1.9	2.2	11.1	9.5	31.6	36.7	92.9

Comparison of the consistency of the tabulated values with experimental data:

- Pre-B cells represent 44% of all B lineage cells and 17% (15.6 % in another study) of all nucleated BM cells (Valenzona *et al.*, 1996).
 - In our table, pre-B cells represent 44.2% of all B lineage cells and 16.1% of all nucleated BM cells.
- B lymphocyte lineage cells represent 38.6% of all nucleated BM cells (Lu and Osmond, 2001).
 - In our table, B lineage cells represent 36.5% of all nucleated BM cells.

- B220⁺ cells constitute 35% of all nucleated BM cells (Lu *et al.*, 1999).
 - In our table, B220⁺ cells constitute 35.79% of all nucleated BM cells.
- The cμ⁺sμ⁻ cells range widely in size, 23% being large cells with diameters of 10-14 μm (Opstelten and Osmond, 1983).
 - In our table, large pre-B cells constitute 23.1% of the compartment.
- Number of cells per femur is 24.5 × 10⁵ for pre-B cells (Park and Osmond, 1987).
 - In our table, the total number of pre-B cells is 26.0 × 10⁵ per femur.
- The incidence of sμ⁺cμ⁻ B cells (% of total nucleated cells) is 15.1 (Opstelten and Osmond, 1983).
 - In our table, the incidence of B cells is 14.4%.

3.1.1.6. Kinetics of Cell Proliferation: DNA synthesis and mitosis are two major events which can reveal kinetic information about dividing cell populations. A main aim of kinetic studies is to find the rate at which individual cells pass throughout the cell cycle to produce two cells, which is the *proliferation rate*, or the *average birth rate*. The proliferation rate (β_i) combined with the population size N_i gives the rate at which new cells are added to the compartment ($\beta_i N_i$). This value can be approximated by the rate of entry into mitosis (r_M) if all cells in the dividing compartment are assumed to be in cycle. i.e., the *growth factor* is unity (100%). Under steady-state conditions and the assumption of random cell loss, this value is equal to the rate at which cells pass at any other point in the cell cycle. The *duration of the cell cycle*, t_C , is the time taken for all cells to pass through any given point in the cell cycle, and is given by the following equation:

$$t_C = \frac{1}{r_M} \quad (3.1)$$

Thus, production rates can also be derived from the measurements of t_C if the labeling index and the average duration of a particular phase are both given. The labeling indices of the DNA synthesis phase and the mitosis phase are frequently used, and are defined as follows:

$$Labeling_index(I_S) = \frac{Average_duration_of_S(t_S)}{Average_duration_of_cell_cycle(t_C)} \quad (3.2)$$

$$Labeling_index(I_M) = \frac{Average_duration_of_M(t_M)}{Average_duration_of_cell_cycle(t_C)} \quad (3.3)$$

Accordingly, t_C can be found by the equation:

$$t_C = \frac{t_S}{I_S} = \frac{t_M}{I_M} \quad (3.4)$$

Since individual cells in a phenotypically defined compartment are not identical, measurements for the cell cycle time t_C actually yield the average apparent cell cycle time $t_{C(a)}$, for the whole population. We will use the term t_C for simplicity. Furthermore, in a closed system, $t_{C(a)}$ also gives the population doubling time (t_D), since it represents the time that all cells pass through a cycle, under the assumption of no cell loss.

The Osmond group used a metaphase arrest (stathmokinetic) technique to quantitate the amount of cell production within proliferating B cell populations in mouse BM. This technique combines metaphase arrest with immunofluorescence labeling, and the proliferation of cells is analyzed under physiological conditions *in vivo* (Opstelten and Osmond, 1983). Administration of vincristine to dividing cell populations is followed with metaphase arrest, and the accumulation of arrested cells with time gives the rate of entry into mitosis. Mean+SD rate of entry into mitosis (r_M) are calculated as follows:

$$r_M = \frac{I_{met}(t_A) - I_{met}(t_0)}{t_A - t_{lag}} \quad (3.5)$$

where I_{met} is the metaphase incidence (the rate of the increase in the percentage of cells in metaphase); and t_{lag} is the time lag after which the drug takes effect, which is established to be 1.3 hours in normal mice (Opstelten and Osmond, 1985).

An example for the metaphase arrest study from the Osmond group is given below for the large and total pre-B cells in Figure 3.2. As can be seen from the figure, the population growth rate is basically estimated as the slope of the linear part of the labeling curve, which is a simplifying assumption. The metaphase incidence I_{met} can be found by taking the average of the initial values on the y-axis: I_{met} for the large pre-B cells and the total pre-B cells is 6.96 and 0.85, respectively.

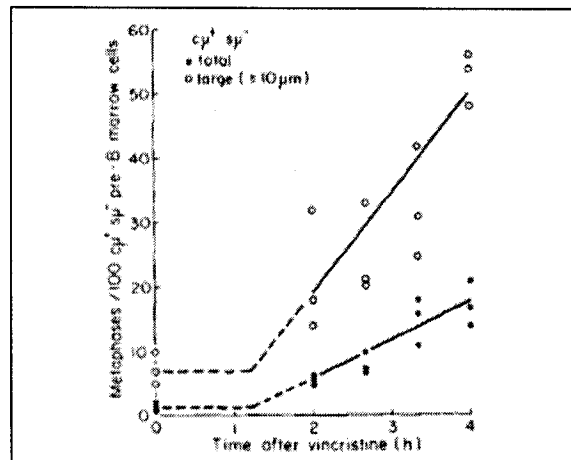


Figure 3.2: I_{met} of pre-B cells after vincristine. The curves were obtained by linear regression analysis of the 12 values for the I_{met} in vincristine-injected mice. The data are derived from three separate experiments (from Opstelten and Osmond, 1983)

The data points in this figure are digitized and the given values for the rate of entry into mitosis are recalculated by fitting a linear curve to the data points. As can be seen from the Figure 3.3, the r_M for the large pre-B and the pre-B compartment as a whole are 15.45, and 6.27, respectively.

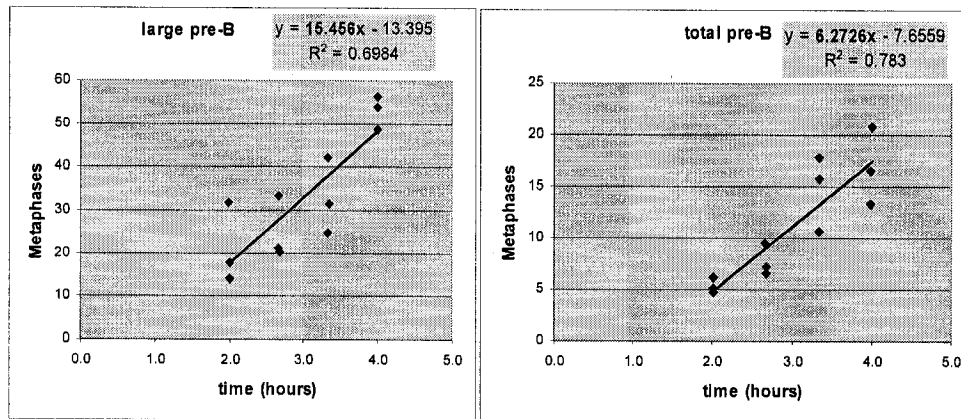


Figure 3.3: I_{met} of pre-B cells (Data from Opstelten and Osmond, 1983- Figure 4,)

The parameter estimates for the kinetics of cell proliferation are summarized below in Table 3.5.

Table 3.5: Parameter values for the kinetics of B cell proliferation in Mouse BM¹

KINETICS OF CELL PROLIFERATION	Pro-B cells			Pre-B cells		B cells	Total
	Early	Int.	Late	Large	Small		
Rate of entry into mitosis (% per hour): r_M	5.1	9.0	14.4*	15.3	n/a	n/a	
	12.5			6.3		n/a	
Apparent average cell cycle time (hours): t_c	19.6	11.1	6.9	6.5	n/a	n/a	
	8.0			15.9		n/a	
Nr of cells produced per femur per hour ($\times 10^4$)	0.6	1.3	10.1	9.2	n/a	n/a	21.2
Nr of cells produced per femur per day ($\times 10^4$)	14.7	30.2	241.9	220.3	n/a	n/a	507.1
Cells produced whole body per day ($\times 10^6$)	2.3	4.8	38.2	34.8	n/a	n/a	80.1

¹ Rate of entry into mitosis is given as a combined value of 13,5% per hour for the intermediate and late pro-B cells and 9% for the intermediate cells only (Park and Osmond, 1989; Osmond *et al.*, 1994). The rate for the late pro-B compartment is calculated by using its respective incidence.

The r_M values are given in percent per hour, and their values are taken from (Park and Osmond, 1989; Opstelten and Osmond, 1983 and Osmond *et al.*, 1994), respectively for the pro-B and the pre-B cells. The average cell cycle times (t_C) are found by $1/r_M$, as stated previously. The total number of cells per femur combined with the r_M gives the number of cells produced per femur per hour, and this value is converted by the factor 15.8 to give the number of cells produced per whole body per day:

$$\frac{\text{Cells}_{-}\text{produced}}{\text{femur} * \text{hour}} (\times 10^4) = \frac{\text{Number}_{-}\text{of}_{-}\text{cells}}{\text{femur}} (\times 10^5) * \frac{r_M}{\text{hour}} / 10 \quad (3.6)$$

$$\frac{\text{Cells}_{-}\text{produced}}{\text{whole}_{-}\text{body} * \text{day}} (\times 10^6) = \frac{\text{Cells}_{-}\text{produced}}{\text{femur} * \text{hour}} (\times 10^4) * 24 * 15.8 / 100 \quad (3.7)$$

3.1.1.7. Kinetics of Cell Turnover: The dynamics of non-dividing lymphocytes can be measured by using the compartment turnover time, which is the time necessary for all cells to be replaced in the compartment. If the compartment is considered to be a “pipeline”, in which all cells spend the same length of time in the compartment, and the first cell in is the first cell out, this results in a linear turnover curve, and its slope provides the turnover time. On the other hand, cells may also leave the compartment at random, which results in an exponentially shaped turnover curve. In this case, the time for fifty percent turnover ($t_{1/2}$) is used instead of the turnover time.

The turnover (or renewal) rate of the nondividing population r_T , together with the population size N , gives the number of cells flowing through the compartment per unit time. If there is no cell loss, this value equals both the inflow rate, and the outflow rate from the compartment. If there is cell loss, this value equals the inflow rate, and the sum of the outflows (\sum_i^o), which are the outflow to the next compartment ($\delta_i N_i$), and the outflow rate of cell loss ($\gamma_i N_i$).

The renewal of nondividing cells is studied by the influx of labeled cells during continuous DNA labeling of all the dividing precursors. The Osmond group used ^3H -thymidine *in vivo* and antiglobulin- ^{131}I binding *in vitro* to determine the development and turnover of immunoglobulin-bearing lymphocytes in mouse BM (Nossal and Osmond, 1974). The ^3H -thymidine labeling indices of the BM small lymphocyte populations are then plotted against time. These indices closely conformed to linear curves on a semi-logarithmic plot, indicating that the real curve is an exponential function of time, and that the transit times are not the same for nondividing lymphocytes. The data are illustrated in Figure 3.4 in terms of the disappearance of unlabeled cells. The time unit is days.

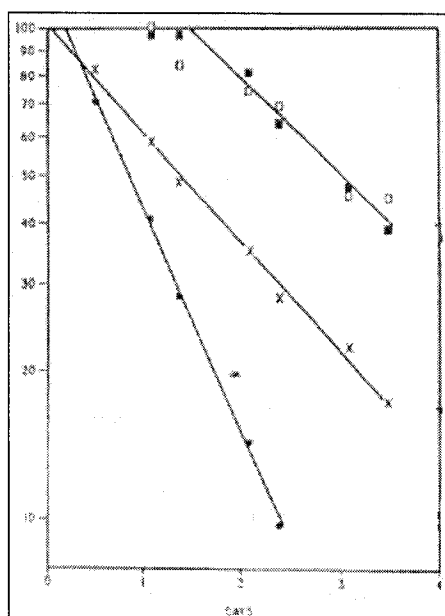


Figure 3.4: Disappearance of cells unlabeled by ^3H -thymidine from the BM of all small lymphocytes (\times), non-Ag-binding small lymphocytes (\bullet) and small lymphocytes binding antiglobulin- ^{131}I in a concentration of $1.0 \mu\text{g/ml}$ (\blacksquare , by observation; \square , by calculation) during repeated administration of ^3H -thymidine *in vivo* (from Osmond and Nossal, 1974)

The non-Ag binding cells ($1.0 \mu\text{g/ml}$) are surface Ig^- small lymphocytes, the great majority being small pre-B cells. Ag-binding cells ($1.0 \mu\text{g/ml}$) are surface Ig^+ small lymphocytes, or simply B cells. The exponential functions fitted to the disappearance of unlabeled cells for small lymphocytes are given in Figure 3.5. Accordingly, the small pre-B cells and the B cells are exponentially renewed with

halving times of 16 hours and 37 hours, respectively (which means that 50% replacement of the B cell population occurs in 37 hours). An example calculation for small pre-B cells is given below:

$$\begin{aligned}
 y(t) &= y(0) * e^{kt} \text{ with } y(0) = 119.77, \text{ and } k = -1.0461 \\
 2 * y(0) &= y(0) * e^{-1.0461 \times t^{1/2}} \\
 2 &= e^{-1.0461 \times t^{1/2}} \\
 \ln(2) &= 1.0461 * t^{1/2} \\
 t^{1/2} &= 0.663 \text{ days} = 16 \text{ hours}
 \end{aligned} \tag{3.8}$$

Since the turnover or renewal rate (% in hour) = $\ln(2) / t_{1/2} * 100$ for nondividing cells, the turnover rates (r_T) for small pre-B cells and B cells are given as 4.36%, and 1.9%, respectively on Table 3.6.

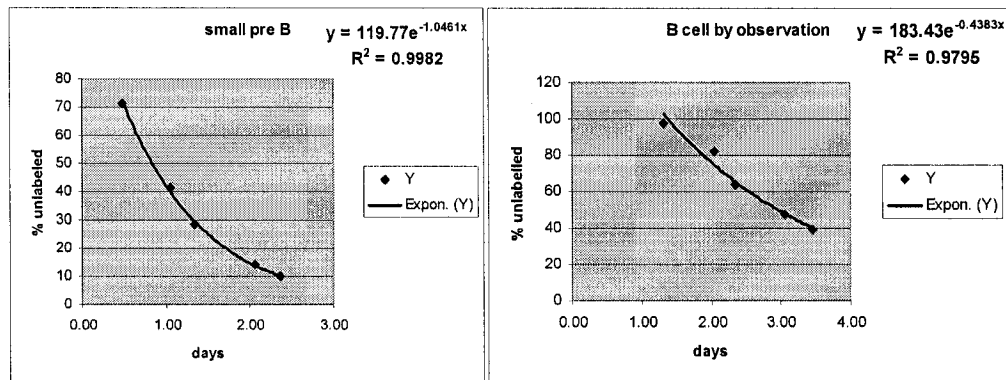


Figure 3.5: Disappearance of unlabeled cells, and the fitted exponential functions for
a) Small pre-B cells and b) B cells

The turnover of small pre-B cells and B cells are found by the following equation:

$$\frac{\text{Turnover_of_cells}}{\text{femur} * \text{hour}} (\times 10^4) = \frac{\text{Number_of_cells}}{\text{femur}} (\times 10^5) * \frac{\text{Turnover_rate}}{\text{hour}} / 10 \tag{3.9}$$

$$\frac{\text{Turnover_of_cells}}{\text{whole_body} * \text{day}} (\times 10^6) = \frac{\text{Turnover_of_cells}}{\text{femur} * \text{hour}} (\times 10^4) * 24 * 15.8/10 \quad (3.10)$$

Table 3.6: Parameter values for the kinetics of B cell turnover in Mouse BM

	Pro-B cells			Pre-B cells		B cells	Total
KINETICS OF CELL TURNOVER	Early	Int.	Late	Large	Small		
Turnover or renewal rate (% per hour): r_T	n/a	n/a	n/a	n/a	4.36	2.00	
Turnover of cells per femur per hour ($\times 10^4$)	n/a	n/a	n/a	n/a	8.72	4.64	13.4
Turnover of cells per femur per day ($\times 10^5$)	n/a	n/a	n/a	n/a	20.93	11.14	32.1
Turnover of cells per whole body per day ($\times 10^6$)	n/a	n/a	n/a	n/a	33.07	17.59	50.7
Number of Mitoses (postulated): M	1	1	3	1	n/a	n/a	6

As can be seen from the table, the turnover of small pre-B cells is much higher than the turnover of the B cells, which itself suggests that a huge number of cells are eliminated at this stage of differentiation. Turnover of the small pre-B cells is around 33 million per day, and 18 million per day for the immature B cells. It is known that only 1-2 million of these cells are released to the periphery, which indicates that another significant portion of the B cells are lost at the B cell stage.

All the parameter values for the kinetics of B cell production and turnover in the BM are listed in Table 3.7

3.1.2. Kinetics of B cell Apoptosis in Mouse Bone Marrow

To evaluate the nature of cell death during normal B lymphopoiesis and its critical stages in mouse BM, the Osmond group examined the kinetics of apoptosis at phenotypically defined stages of B cell differentiation. Apoptotic cells are identified by both electron microscope morphology and evidence of DNA fragmentation.

Immunofluorescence labeling and flow cytometry were used to quantitate phenotypically defined B cell populations and to examine their *ex vivo* incidence of apoptosis and the *in vitro* relative rate at which cells enter apoptosis at phenotypic stages of B cell differentiation (Lu and Osmond, 1997). Then, the experiment is

repeated for the comparison of the susceptibility of precursor B cells to induction of apoptosis by dexamethasone (Dex), and to protection of stromal cell coculture.

In this study, we used these two parameters, i.e. the apoptotic index (I_{apop}), and the apoptotic rate (γ_i), to estimate the true magnitude of apoptosis. Figures 3.6 and 3.7 depict the incidence of hypodiploid cells at various phenotypic stages of B cell development, and the rate at which the frequency of apoptotic cells increases during 0-8 hour periods of incubation *in vitro*, respectively.

Since apoptotic cells are rapidly recognized and engulfed by BM macrophages, the number of hypodiploid cells detectable at any given time is small. Thus, the incidence of apoptosis alone cannot accurately assay the true magnitude of apoptosis, but it has the advantage of being an *in vivo* measurement.

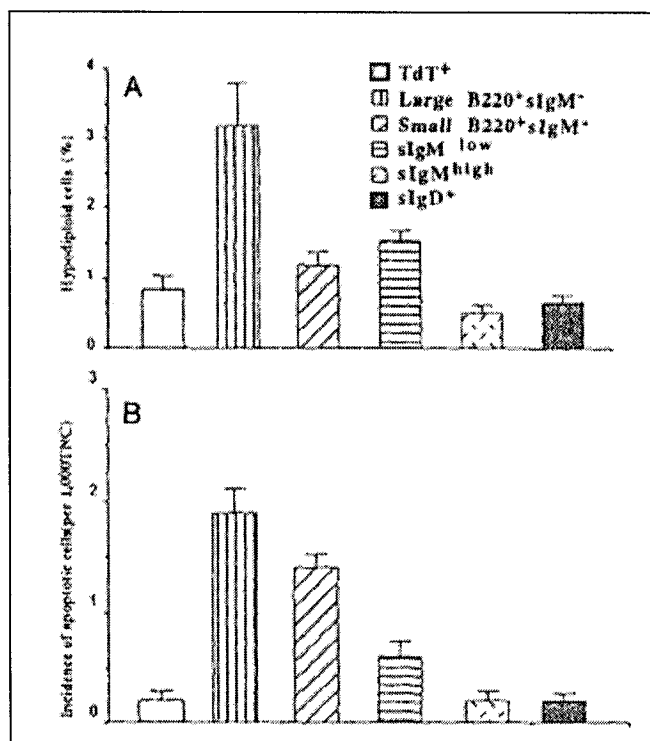


Figure 3.6: Incidence of hypodiploid cells at various phenotypic stages of B cell development in freshly prepared BM cell suspensions detected by flow cytometry.

A, Incidence of apoptotic B cells within each defined compartment.

B, Frequency of apoptotic B cells per 1000 total nucleated BM cells. Data were derived from four separate experiments (mean \pm SD) (from Lu and Osmond, 1997)

On the other hand, apoptotic cells increase linearly with time without macrophage ingestion during short term culture *in vitro*, which provides a direct assay for the rate of entry into apoptosis, linearity being the major assumption. This rate at which cells of a given compartment enter apoptosis can be combined with the total number of cells in this phenotypic compartment to give an estimate for the actual number of cells entering apoptosis per unit time.

Alternatively, the numerical ratio between the apoptotic index (%) and apoptotic rate (%/h) can be used to estimate apoptosis by multiplying it with the *ex vivo* apoptotic index. This ratio is approximately consistent, and is given as 1.9 for the precursor B lymphocytes (Lu and Osmond, 2000). In our study, we will consider and compare both of these approaches.

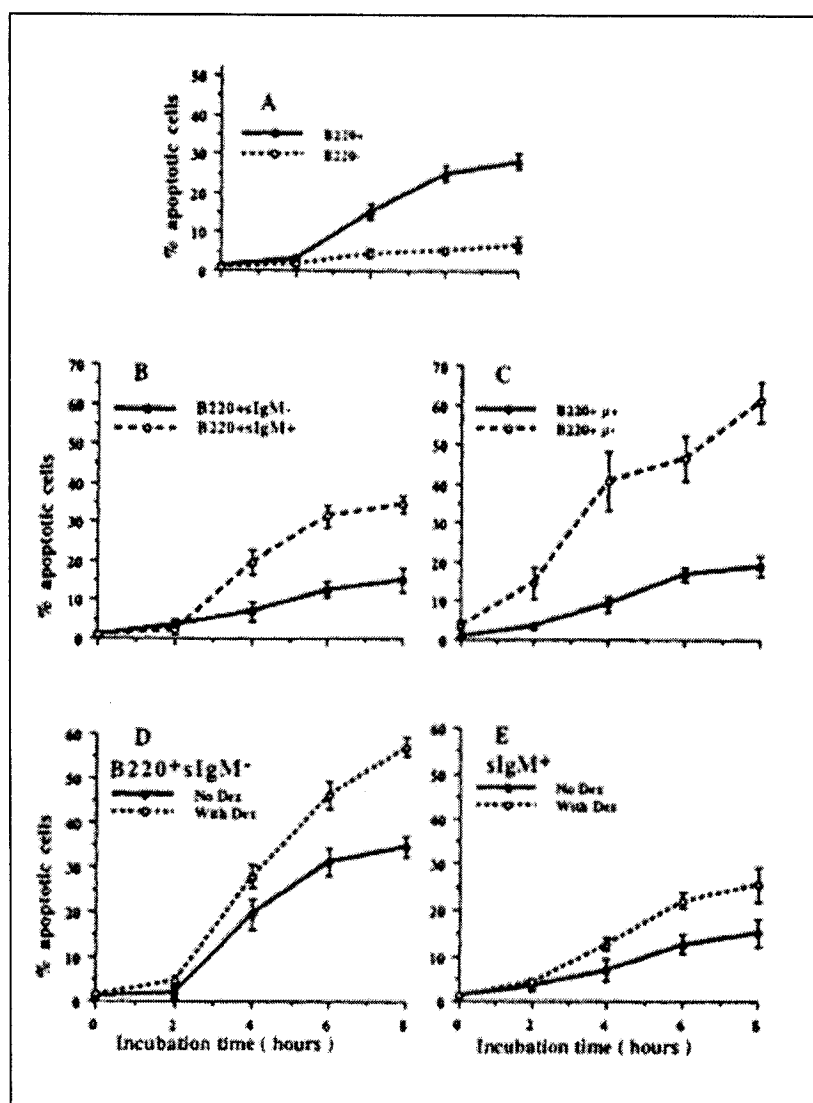


Figure 3.7: Incidence of hypodiploid cells, detected by flow cytometry in mouse BM suspensions during 0- to 8-h incubation.

- A, Comparison of apoptosis among B220⁺ B lineage vs B220⁻ non-B lineage cells,
 B, Comparison of apoptosis among B220⁺slgM⁻ precursor B vs slgM⁺ B lymphocytes,
 C, Comparison of apoptosis among B220⁺μ⁻ pro-B vs B220⁺μ⁺ cells.
 D and E, Comparison of apoptosis within B220⁺slgM⁻ and slgM⁺ populations when incubated either with or without 1 μM of Dextran. Data represents four separate experiments (mean ± 2 SD) (from Lu and Osmond, 1997)

Moreover, there is another set of experiments in which apoptosis of precursor B cells is modified by co-culture with stromal cells. It is seen that the incidence of hypodiploid B lineage cells were decreased in the presence of stromal cells when compared with cells cultured in medium alone. However, precursor cells and B

lymphocytes were affected differently. The apoptotic index of $B220^+sIgM^-$ cells was reduced considerably after coculture with stromal cells (from 27.8 to 13.9%), and the apoptosis rate was approximately halved ((from 4.3%/h to 2.3%/h). On the other hand, the apoptotic index of $sIgM^+$ cells exhibited less reduction (from 14.7 to 10.9%), and apoptotic rate did not change appreciably (1.8%/h) (Lu and Osmond, 1997). The conditions of stromal cell co-culture are closer to in-vivo conditions than the in-vitro measurements without stromal cells, and will be taken into account. Although the exact values are not given for all phenotypically defined compartments, the apoptosis rate given by the *in vitro* measurement for the precursor B cells is approximately halved in the presence of stromal cells. The change in the apoptotic rates with and without stromal cell support is shown in Figure 3.8.

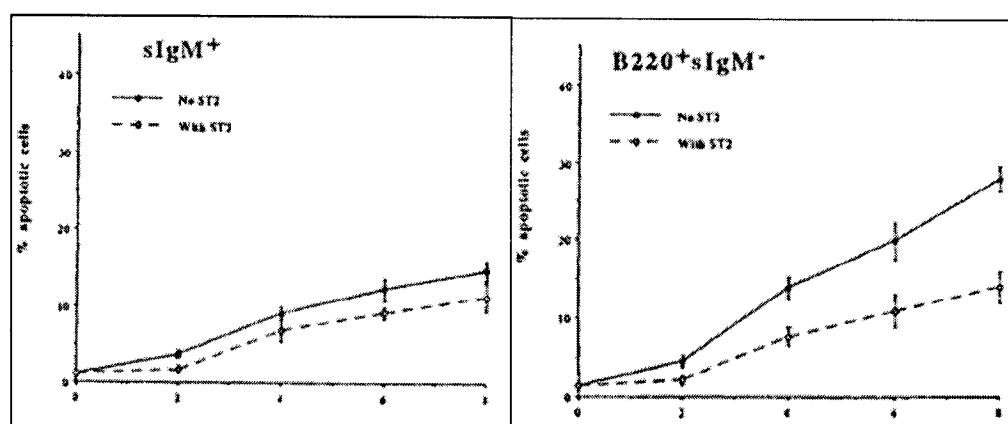


Figure 3.8: Incidence of hypodiploid cells detected by flow cytometry in mouse BM suspensions during 0- to 8-h incubation (given in hours) with or without a monolayer of stromal cells. Data represent three separate experiments (mean \pm SD) (from Lu and Osmond, 1997).

All the parameter values for B cell apoptosis in the BM are listed in Table 3.8. Two different sets of values are given for the apoptotic rate. One belongs to *in vitro* measurements, and the other is estimated by using the apoptotic incidence, as mentioned previously.

The apoptosis rate combined with the total number of cells gives an estimate the number of cells entering apoptosis per hour per femur in that compartment, as mentioned previously and, by extrapolation, in the whole body bone marrow volume.

Table 3.7: Summary of the parameter values for the kinetics of B cell production and turnover in BM

Kinetics of B Cell Production in Bone Marrow							
	Pro-B cells			Pre-B cells		B cells	Total
MICE 7-10 weeks, CH HeJ, C57Bl/6 and CB/Alc Wehi strains	Early	Int.	Late	Large	Small		
CELL MARKERS							
Terminal deoxynucleotidyl Transferase (TdT)	xxxxxx	xxxxxx					
B220		xxxxxx	xxxxxx	xxxxxx	xxxxxx	xxxxxx	
Cytoplasmic μ chains (cp)				xxxxxx	xxxxxx		
Surface immunoglobulin M (sIgM)						xxxxxx	
KINETIC STATE							
Dividing (in cell cycle - G1, S, G2, M)	xxxxxx	xxxxxx	xxxxxx	xxxxxx			
Non dividing (not in cell cycle - G0)					xxxxxx	xxxxxx	
CELL SIZE							
range (μ m)	7-13			10-14	7-10		
cell size (μ m)	9.0	10.0	12.0	12.0	8.0	8.0	
POPULATION SIZE							
	0.7	0.9	4.3	3.7	12.4	14.4	36.5
Incidence (% of total nucleated cells) in BM	6.0			16.1			
	2.0	2.4	11.9	10.2	34.0	39.5	100.0
Incidence (% of B lineage cells) in BM	16.3			44.2			
Number of cells per femur ($\times 10^5$): N	1.2	1.4	7.0	6.0	20.0	23.2	58.8
KINETICS OF CELL PROLIFERATION							
	5.1	9.0	14.4	15.3	n/a	n/a	
Rate of entry into mitosis (% per hour): r_M	12.5			6.9		n/a	
	19.6	11.1	6.9	6.5	n/a	n/a	
Apparent average cell cycle time (hours): t_c				15.9		n/a	
Number of cells produced per femur per hour ($\times 10^4$)	0.6	1.3	10.1	9.2	n/a	n/a	21.1
KINETICS OF CELL TURNOVER							
Turnover or renewal rate (% per hour): r_T	n/a	n/a	n/a	n/a	0.00	0.00	
Turnover of cells per femur per hour ($\times 10^4$)	n/a	n/a	n/a	n/a	0.0	0.0	
Number of Mitoses (postulated): M	1	1	3	1	n/a	n/a	6

Table 3.8: Summary of the parameter values for the kinetics of B cell apoptosis in BM

		2.1				
		1.4				
			1.6			
			3.5	0.8		
Apoptotic rate estimated from incidence (% per hour)		1.5		0.0	2.3	2.9
	1.5					
		3.8		2.3		
		4.0				
		2.7				
KINETICS OF APOPTOSIS						
		9.0		3.8		1.8
	0.0	3.0	10.0	4.9		
Rate of entry into apoptosis (% per hour):		9.0		8.3	2.4	1.8
		7.3				1.8
		4.7		8.3		1.8
		5.3				
Outflow rate of entry into apoptosis cells/hour/femur) (10 ⁴)	0.36	0.70	7.00	4.98	4.08	4.18
Outflow rate of entry into apoptosis cells/day/whole body BM) (10 ⁶)	1.19	2.65	26.54	18.88	15.47	15.84

3.2. Rat Data- Opstelten Scheme

In this part of the study, we will use the data which is collected by Dr. Opstelten and her coworkers. Dr. Opstelten is one of the former coworkers of Prof. Osmond, and her group used the same techniques that are previously used to characterize the B cell sequence in the mouse BM. Using a combination of metaphase arrest technique and immunofluorescence staining, they characterized a B cell differentiation sequence in the rat BM, which is based on the expression of particular molecules with time (Deenen *et al.*, 1987):

- 1) Terminal deoxynucleotidyl transferase (**TdT**), expressed in the cell nucleus during immunoglobulin heavy (IgH) chain gene rearrangement
- 2) **HIS24** cell surface glycoprotein (analogous to **B220** in mouse)
- 3) μ chains in cytoplasm (**c μ**), and
- 4) μ chains in IgM molecules expressed at cell surface (**s μ** , **sIgM**)

These four markers define successive stages in B cell development. The earliest defined precursor B cells are called HIS24 cells, which is comprised of two populations of proliferating and nonproliferating cells before the expression of μ chains. The subsequent populations comprise TdT⁺ cells and pre-B cells, which give rise to nondividing B lymphocytes expressing surface IgM. These stages are assumed to form a series of concatenated compartments, (except that it is not known if TdT is an obligatory stage in B cell genesis) the 'outflow' from one compartment being the 'inflow' to the next compartment:

- 1) HIS24 cells: Small (HIS24⁺)
Large (HIS24⁺)
- 2) TdT cells: Small (TdT⁺, HIS24⁺, c μ ⁺)
Large (TdT⁺ HIS24⁺, c μ ⁺)
- 3) B cells: Small (HIS24⁺, sIgM⁺)
Large (HIS24⁺, sIgM⁺)

3.2.1. Kinetics of B cell Production in Rat Bone Marrow

3.2.1.1. Age and Strain: To minimize variations in collected data as much as possible, the analysis of Opstelten group has been restricted to data sets which belongs to the AO/G \times BN/ G) F₁ hybrid rats, at the age of either 5-6 weeks or 10-12 weeks. Here we will present the data which belongs to the second group only since this data set is more complete and 10-12 weeks is the age of the average age of an adult rat, so the BM cell populations can be assumed to have reached their steady state levels.

3.2.1.2. Cell Markers: The table 3.9 summarizes the cell markers associated with the B lineage, and correlates them with the related stages of B cell development:

Table 3.9: Cell markers of the phenotypically defined B cell compartments in Rat BM

	HIS24		TdT		Pre-B		B	
CELL MARKERS	Small	Large	Small	Large	Small	Large	Small	Large
TdT			xxxx	xxxx				
HIS24 (instead of B220)	xxxx	xxxx	xxxx	xxxx	xxxx	xxxx	xxxx	xxxx
Cytoplasmic μ chains (c μ)					xxxx	xxxx		
Surface IgM (sIgM)							xxxx	xxxx

3.2.1.3. Kinetic State: The kinetic state of the precursor B compartments is summarized in Table 3.10. Accordingly, all the large HIS24, TdT, Pre-B and B cells are in cell cycle (G₁, S, G₂, or M), and all the small cells in these compartments are not in cycle (in G₀).

Table 3.10: Kinetic state of the phenotypically defined B cell compartments in Rat BM

	HIS24		TdT		Pre-B		B	
KINETIC STATE	Small	Large	Small	Large	Small	Large	Small	Large
Dividing (in cell cycle)		xxxx		xxxx		xxxx		
Nondividing (in G ₀)	xxxx		xxxx		xxxx		xxxx	xxxx

3.2.1.4. Cell Size: The cell size (given in modal cell diameters), and range of the phenotypically defined precursor B cells are listed in Table 3.11. In our analysis, the cell size data is not used. However, it can be suggested that for every phenotypically defined cell compartment, the compartment boundary between the large and the small cells is defined by mitosis, since mitosis are confined to subsets of large cells.

Table 3.11: Parameter values for the cell size in Rat BM

	HIS24		TdT		Pre-B		B	
CELL SIZE	Small	Large	Small	Large	Small	Large	Small	Large
cell size (μm)	<11	≥ 11	<11	≥ 11	<12	≥ 12	<12	≥ 12
range (μm)	7-21		9-18		7-18		7-18	
modal diameter (μm)			10.5		9.5		9.5	

TdT⁺ and pre-B cells range between 7 and 18 μm in diameter, and TdT⁺ cells tend to be larger than the pre-B cells (modal cell diameters of 10.5 μm and 9.5 μm) (Opstelten *et al.*, 1986). Similarly, most of the B cells in cytocentrifuge preparations were small, 7 to 11 μm in cell diameter, with a modal cell size of 9.5 μm (Deenen *et al.*, 1987).

3.2.1.4. Population Size: The population size of the precursor B cells in the rat BM is determined by obtaining different subsets with immunofluorescence staining and multiplying by the total cell count, which gives the total number of cells per femur for a given phenotypically defined compartment. This value can be converted by the estimated ratio of the total number of cells in the BM to the number in one femur. There is a single estimate for this ratio (32.2), which likely varies between individual rats and between different rat strains, but nevertheless is used in all calculations in this study to give an estimate for the whole body size of each cell population.

All the parameter values related to the population size are tabulated in Table 3.12. In the first two rows; the incidences are given in terms of the percentage of total nucleated cells, and of B lineage cells in the rat BM. The relative incidence in the group is given in the third row. The number of cells per femur and per whole body BM is given in the last two rows. Since there are two independent studies with estimations of population size, the mean of the available estimations are used in this table, or the best one is chosen according to the strain and age. The values for the table are taken from (Deenen *et al.*, 1990 and Deenen *et al.*, 1987).

Moreover, the size of the defined cell groups is modified according to the following observations of the Opstelten group:

- HIS24⁺ compartment shows a phenotypic heterogeneity. Six percent of TdT⁺ cells express μ chains and are therefore pre-B cells, and therefore subtracted from the TdT compartment
- Twenty percent of HIS24⁺TdT⁺ μ ⁻ cells express Ig other than μ chains, therefore these cells are excluded from the HIS24 compartment.

Table 3.12: Parameter values for the population size of B cells in Rat BM

	HIS24		TdT		Pre-B		B		Total
POPULATION SIZE	Small	Large	Small	Large	Small	Large	Small	Large	
Incidence (% of total nucleated cells) in BM	2.10	2.70	2.10	0.70	11.90	4.50	3.50	0.60	
	4.80		2.80		16.40		4.10		28.10
Incidence (% of B lineage cells) in BM	7.00	10.83	5.91	2.44	43.33	16.80	11.76	1.91	
	17.84		8.36		60.13		13.68		100.00
Relative incidence in the group (%)	39.26	60.74	70.77	29.23	72.07	27.93	86.00	14.00	
	100.00		100.00		100.00		100.00		
Number of cells per femur ($\times 10^6$)	2.56	3.96	2.16	0.89	15.84	6.14	4.30	0.70	
	6.52		3.06		21.98		5.00		36.56
Number of cells per whole body BM ($\times 10^7$)	21.00		9.80		70.80		19.90		121.50

3.2.1.5. Kinetics of Cell Proliferation: Parameters which define the kinetics of cell proliferation is calculated similarly as we did in the previous chapter, and are depicted below in Table 3.13. Rate of entry into mitosis is only defined for proliferating large compartments except immature B cells, since there were no significant metaphases in μ ⁺ cells. The average apparent cell cycle time is found by dividing 100 by the rate of entry into mitosis, and then the number of cells per femur and per whole body marrow is calculated.

An example for the metaphase arrest study from the Opstelten group is given below for the large HIS24, TdT and pre-B cells in Figure 3.9. As can be seen from the figure, the population growth rate is estimated as the slope of the linear part of the labeling curve, which is a simplifying assumption. The metaphase incidence I_{met} can be found by taking the average of the initial values on the y-axis: I_{met} for the large HIS24 cells, TdT cells a pre-B cells is 7.0, 5.8 and 5.5, respectively.

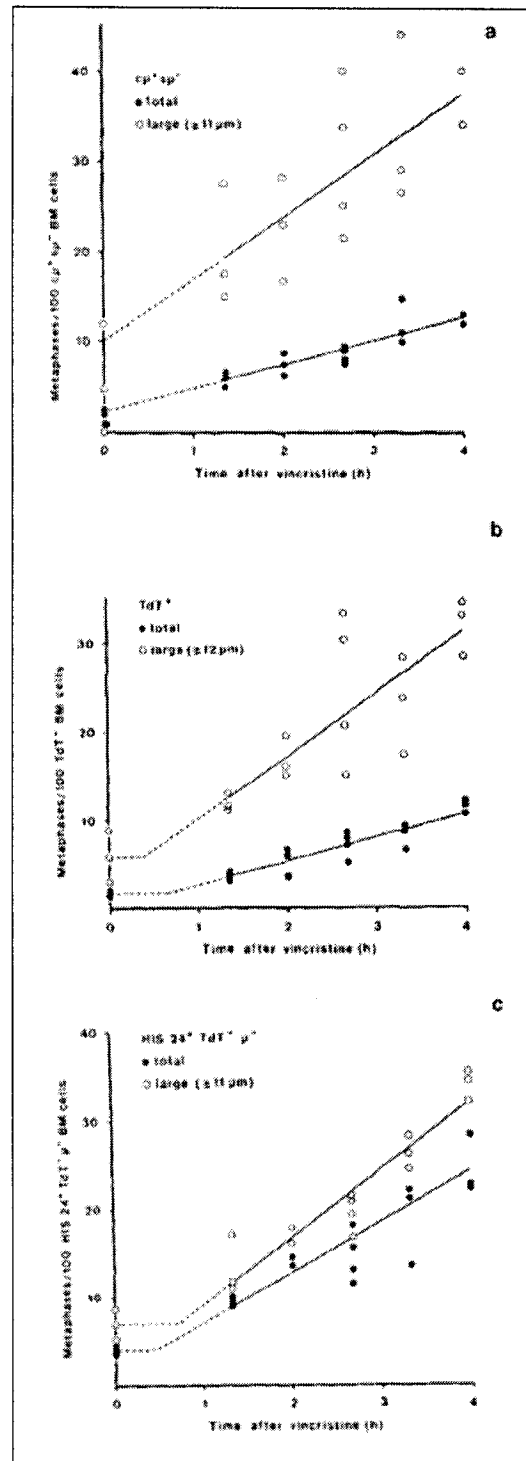


Figure 3.9: I_{met} of HIS24⁺ BM cell subsets after vincristine. The lines were obtained by linear regression analysis of 15 (cp^+sp^- , HIS24⁺TdT⁺μ⁻) or 16 (TdT⁺) values for I_{met} in vincristine-injected rats (from Deenen, Hunt and Opstelten, 1987)

Table 3.13: Parameter values for the kinetics of B cell proliferation in Rat BM

	HIS24		TdT		Pre-B		B		Total
KINETICS OF CELL PROLIFERATION	Small	Large	Small	Large	Small	Large	Small	Large	
Rate of entry into mitosis (% per hour)	n/a	7.50	n/a	6.80	n/a	6.70	n/a	n/a	
	5.20		2.80		2.60		n/a		
Apparent average cell cycle time (hours)	n/a	13.33	n/a	14.71	n/a	14.93	n/a	n/a	
	19.23		35.71		38.46		n/a		
Nr of cells produced per femur per hour ($\times 10^4$)	n/a	29.6	n/a	6.10	n/a	41.10	n/a	n/a	
	33.90		8.50		58.00		n/a		100.40
Nr of cells produced per femur per day ($\times 10^5$)	n/a	71.09	n/a	14.64	n/a	98.64	n/a	n/a	
	81.36		20.40		139.20		n/a		240.96
Cells produced per whole body per day ($\times 10^7$)	n/a	22.90	n/a	4.70	n/a	31.80	n/a	n/a	

3.2.1.6. Kinetics of Cell Turnover: The renewal of nondividing cells is studied by the influx of labeled cells during continuous DNA labeling of all the dividing precursors. The Opstelten group used BrdUrd *in vivo* fluorescence microscopy to determine the development and turnover of immunoglobulin-bearing lymphocytes in rat BM (Deenen *et al.*, 1990). The BrdUrd labeling indices of the BM small lymphocyte populations are then plotted against time. These indices closely conformed to linear curves on a semi-logarithmic plot, indicating that the real curve is an exponential function of time, and that the transit times are random for nondividing lymphocytes. The data are illustrated in Figure 3.10 in terms of the disappearance of unlabeled cells. The time unit is hours.

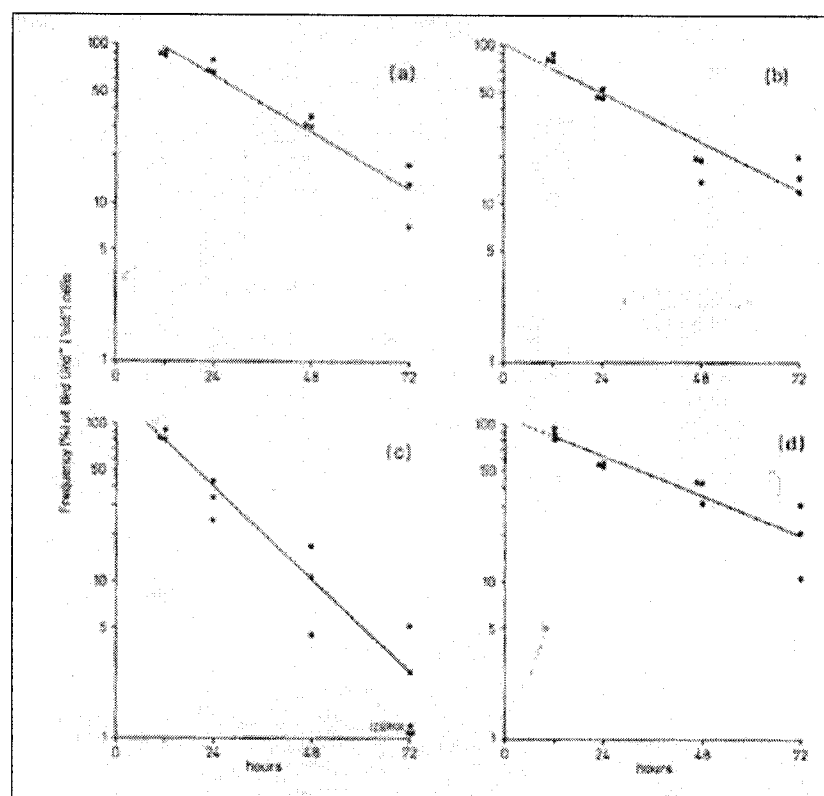


Figure 3.10: Disappearance of cells unlabeled (BrdUrd-) sIgM+ B lymphocytes and small B precursor cells in rat BM during continuous infusion of BrdUrd. (a) sIgM+ B lymphocytes; (b) small (<11 μm) pre-B cells; (c) small (<12 μm) TdT+ cells; (d) small (<11 μm) HIS24+TdT-Ig- cells (*from Deenen, Balen and Opstelten, 1990*)

The turnover rates (r_T) for small HIS, TdT, pre-B and B cell compartments are calculated as 2.39, 5.64, 2.98 and 3.45 respectively and can be seen in Table 3.14.

Table 3.14: Parameter values for the kinetics of B cell turnover in Rat BM

	HIS24		TdT		Pre-B		B	
KINETICS OF CELL TURNOVER	Small	Large	Small	Large	Small	Large	Small	Large
Turnover or renewal rate (% per hour)	2.39	n/a	5.64	n/a	2.98	n/a	3.45	
Turnover of cells per femur per hour ($\times 10^4$)	6.1	n/a	12.2	n/a	47.2	n/a	20.0	
Turnover of cells per whole body per day ($\times 10^6$)	47	n/a	94	n/a	365	n/a	155	

4. PROBLEM DESCRIPTION AND RESEARCH OBJECTIVE

The definition, kinetic properties and regulation of the subpopulations of progenitors and non-dividing progeny in bone marrow lymphopoiesis remain less well understood than in the parallel processes of erythrocytopoiesis and granulocytopoiesis. Moreover, the marrow lymphoid cells are functionally heterogeneous (Miller *et al.*, 1973), and the use of diverse phenotypic criteria and terminologies in different laboratories has led to the formulation of disparate models of lymphopoiesis that are not fully consistent with each other. This factor has been recently resolved by Dennis Osmond, Antonius Rolink and Fritz Melchers who combined their findings to provide a common phenotypic model of B-cell development in mouse BM and provide a common reference database (Osmond *et al.*, 1998). Another factor that hampers cross-reference between various models of B lymphopoiesis is that the results of different studies to quantify the populations of subpopulations of B cells in mouse BM vary greatly due to differences between mouse strains, the use of different markers, variability in experimental conditions or differences in the methods used to calculate the final numbers. Many studies use the percentages of cells in different subsets in BM (obtained by flow cytometry) from one or two femura, multiplied by the total cell count.

To sum up, both the differences in final cell counts of different experiments and techniques, and the differences in methods and their applicability to the given blood cell lineage, in particular B cell differentiation, are challenging for biologists, in part due to the complex nature of the haematopoiesis.

While the study of the differentiation and development of the B cell subsets is of clear importance in immunology, the homeostatic mechanisms for lymphocyte development remain elusive. In the adult mouse and rat, the number of B and T lymphocytes remains constant in spite of continuous production and peripheral cell division; however the mechanisms that govern the number of lymphocytes in the BM, thymus and the periphery are poorly understood.

In this context, mathematical models act as a useful tool to analyze hypotheses and experiments concerning mechanisms of steady state numbers of B and T lymphocytes. These models can make a significant contribution to the current understanding of lymphocyte differentiation by revealing some of the crucial parameter values for the system at steady state. Also, models provide an experimental platform for simulating known conditions. The simulation results can be compared to experimental data.

Several mathematical analyses exist which model different aspects of B and T cell differentiation, however little attempt has been made to model the B cell development in the BM, except for the recent work of Mehr et al. (2003). The goal of this study is to develop a mathematical model for the proliferation and differentiation of mammalian B lymphocytes in laboratory mice and rats. The first step towards this objective is to make an extensive summary of all the existing data on the various B cell precursors (for mice and rats) and organize it into a comprehensible and consistent framework. Then this final data set will be used to estimate all of the parameters to explain the existing steady state data, to find (if there is any) the parameter sets which are consistent with the given experimental results for B cell populations and their measured proliferation and turnover kinetics.

The final set of steady state parameters can reveal answers for some of the crucial questions regarding the kinetics of B cell development, apoptosis and the unified model of B cell production and loss. There are a number of immunologically important parameters which are difficult to measure experimentally, but can be determined by various mathematical approaches. As for B cell development, the parameters of interest are the calculated steady state flows from compartment to compartment, the daily output of B cells from the BM and the flow from stem cell precursors. Other important parameters which can be derived using the steady state data include the number of mitoses within each compartment, cell cycle parameters such as cell cycle duration, length of elapsed time from Early Pro-B cell to B cell stage, and the number of cells per clone. We can also assess the effect of reducing or eliminating the Late Pro-B cell stage to test the relevancy of the late pro-B cell compartment. As for B cell apoptosis, we can find the number of cells that are

eliminated per unit time in each compartment, the total magnitude of cell loss by apoptosis, and the main checkpoints at which cells are triggered into apoptosis.

A unified model of B cell production and loss gives us information about the correlation of values for cell production and cell loss and estimates for the daily output of B cells from BM, the number of clones per day, and the number of cells per clone. We can test the effect of varying the proliferative kinetic and apoptotic rates on B cell output at particular points during B cell development, or test for the presence of the hypothetical phenotypic “reflux” from the B cell compartment to the Pre-B cell compartment (due to Receptor Editing).

The model that we develop to explain these steady state data can then be used to predict temporal responses to various experimental perturbations by employing a homeostatic feedback model, similar to previous mathematical T cell models, in which the growth rate is defined as a nonlinear relationship of population size and in which there exist a predefined “carrying capacity”. For T cells, the carrying capacity refers to the maximum number of cells that is assumed to exist in the thymus, based on data indicating that the total number of thymocytes is autonomously controlled (Metcalf, 1963).

5. DESCRIPTION OF MODEL

In our analysis, we will regard any phenotypically defined cell populations as virtual “compartments”, through which individual cells should pass with time in the course of their maturation in the BM. Those compartments are not to be confused with physical spaces; however the physical pathway of the individual cells throughout their development in the BM can also be introduced as an additional dimension in a more sophisticated model. First, we will assume these stages to form a series of concatenated compartments and try to see if the unidirectional flow assumption yields feasible results for steady-state flows between compartments, then we will try to see if the data still yields positive values if we postulate a bi-flow between small pre-B and B cells due to the recent hypothesis of “receptor editing”.

The number of cells of a particular type in a compartment i at time t , and the output of cells to the next compartment depend on some potentially variable parameters, including the cell input from the preceding compartment, the proliferative activity within the compartment (number of mitotic cell cycles, length of cell cycle, growth fraction), the loss of cells due to death and/or emigration from the compartment (if postulated), and the speed of differentiation, i.e. the time necessary for the cells to acquire phenotypic properties of the next compartment (Osmond *et al.*, 1998). More specifically:

The sum of the inflows equals sum of the outflows for any given compartment i , where sum of inflows is defined by the summation of proliferation and cells entering from the previous compartment, and sum of outflows is defined by cells entering the next compartment, and proliferation:

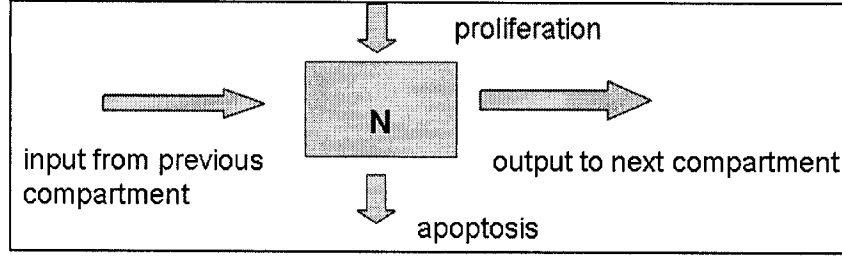


Figure 5.1: Flows for a hypothetical compartment of size N

$$\sum_i^i = \sum_i^o, \quad (5.1)$$

$$\text{where } \sum_i^i = \beta_i N_i + \delta_{i-1} N_{i-1} \quad (5.2)$$

$$\text{and } \sum_i^o = \delta_i N_i + \gamma_i N_i \quad (5.3)$$

In a proliferating compartment, the relationship between the input and the output rate can be defined as follows, assuming there is no cell loss:

$$\text{output_rate} = 2^M * \text{input_rate} \quad (5.4)$$

If there is cell loss, output will be equal to the sum of output to the next compartment, and apoptosis, which equals to the sum of proliferation and the input from the previous compartment, according to Eq. 3.5. The modified equation will become:

$$\text{input_rate} + \text{proliferation} = 2^M * \text{input_rate} \quad (5.5)$$

Since we calculated all the flows between the compartments, the number of mitotic cycles within a compartment, M_i , can be found by using this equation, and it follows that:

$$M = \frac{\ln\left(\frac{\text{input_rate} + \text{proliferation}}{\text{input_rate}}\right)}{\ln(2)}, \text{ which equals to}$$

(5.6)

$$M = \frac{\ln\left(\frac{\delta_{i-1} * N_{i-1} + \beta_i * N_i}{\delta_{i-1} * N_{i-1}}\right)}{\ln(2)} \quad (5.7)$$

5.1. Summary of Parameters and Flows for Mice

Starting with immature B cells, we calculated back up to early pro-B cells using the above rules, where the balance of inflows- outflows is forced to be zero. Accordingly, steady state flows and parameters can be found, which are subject to change especially due to the high variability in apoptotic rate estimates.

The Table 5.1 summarizes the flows between compartments calculated with the given kinetic parameters (See Table 3.7 and Table 3.8 in Chapter 3) and the resulting number of mitoses in each proliferating compartment. Accordingly, the values for the flows are given in 10^4 cells per femur per hour, and the totals are also given when appropriate. It should be noted that this table represents only one feasible data set which is consistent with the given kinetic parameters and with each other, and there is a feasible *range* of parameter sets which gives non-zero values for the estimated flows and the corresponding number of mitoses.

Accordingly, the magnitude of cell input from the immediately preceding compartment of the early pro-B cells is in the order of 2 million per day (See Table 5.2 first row), which corresponds to the steady-state number of cells which are expected to arise from the stem cell lymphocyte compartments to feed the precursor B cells. The estimated outflow from the BM to the peripheral compartments is found as 1.8 million cells per day, which is quite comparable to the previous estimates of the Osmond group given as 1-to 2 million cells per day. The number of mitotic cycles are estimated as 1, 1.3, 3, and 1.6 in the pro-B and large pre-B compartments, which gives

a cumulative number of ~ 7 for the total number of mitotic cycles in the B cell lineage in BM, which is again comparable to the postulate of 6 of the Osmond group.

The total number of mitotic cycles gives an important information about the “clone size”. Clone size gives the number of cells that have an identical antigen binding receptor, i.e. their Ig molecules are identical with each other. If the total number of mitoses is 6, the maximum number for the clone size will be $2^6 = 64$ (There are many of these clones, but there is only 64 entering the bloodstream having the same antigen binding specificity). Accordingly, the average clone size in mice B cell is around 120.

From the table it can also be seen that ~ 80 million cells are produced each day in the BM to feed the B lymphocyte precursors, however the cells that are lost due to apoptosis are also in the same order of ~ 80 million. At the end of this battle for survival, only ~ 2 million of the B cells can leave the BM and enter the bloodstream. This can be an indication for the assurance of the high quality check for the peripheral B lymphocytes, since more than 90% of the B lymphocytes produced in the BM are destined to die before entering the bloodstream even in the steady state conditions.

Table 5.1: Summary of flows between compartments and number of mitoses-for Mouse

	Pro-B cells			Pre-B cells		B cells	Total
FLows BETWEEN COMPARTMENTS ($\times 10^4$ cells/femur/hour)	Early	Int.	Late	Large	Small	Immature	—
Inflow from previous compartment	0.63	0.88	1.44	4.52	8.72	4.64	—
Inflow proliferation	0.61	1.26	10.08	9.18	0.00	0.00	21.13
Outflow to the next compartment	0.88	1.44	4.52	8.72	4.64	0.46	—
Outflow apoptosis	0.36	0.70	7.00	4.98	4.08	4.18	21.30
Sum of inflows	1.24	2.14	11.52	13.70	8.72	4.64	—
Sum of outflows	1.24	2.14	11.52	13.70	8.72	4.64	—
Balance (should be zero)	0.00	0.00	0.00	0.00	0.00	0.00	—
MITOSES							
Number of mitoses	0.98	1.28	3.00	1.60	n/a	n/a	6.86

Table 5.2: Daily flows between compartments-for Mouse

	Pro-B cells			Pre-B cells		B cells	Total
FLows BETWEEN COMPARTMENTS ($\times 10^8$ cells/whole body BM/day)	Early	Int.	Late	Large	Small	Immature	—
Inflow from previous compartment	2.08	3.34	5.46	17.14	33.07	17.59	—
Inflow proliferation	2.03	4.78	38.22	34.81	0.00	0.00	79.84
Outflow to the next compartment	2.92	5.46	17.14	33.07	17.59	1.76	—
Outflow apoptosis	1.19	2.65	26.54	18.88	15.47	15.84	80.58
Sum of inflows	4.11	8.11	43.68	51.95	33.07	17.59	—
Sum of outflows	4.11	8.11	43.68	51.95	33.07	17.59	—
Balance (should be zero)	0.00	0.00	0.00	0.00	0.00	0.00	—

5.2. Summary of Parameters and Flows for Rat

The same techniques are applied to the rat data set, and the estimates for the flows between the compartments and the mitotic cycles are listed in Table 5.3. As the Opstelten group did not provided any absolute final scheme for the B cell differentiation in rat BM and mentioned that other combinations are also possible (Deenen *et al.*, 1990), we also considered the possibility that the cells can be fed by all their previous compartments, and not only by the imminent previous compartment. The other shortcoming of the rat data is we do not have any estimates for the apoptosis rates unlike the mice data, which restricts our analysis. However we postulated an outflow for apoptosis to see if we can find any estimates for the true rate of cell loss of the rat B cell lineage.

It must be noted that according to this scheme, HIS24 cells correspond to $\text{HIS24}^+\text{TdT}^-\mu\text{Ig}^-(\text{H}+\text{L})^-$ cells, likely to represent the true progenitors. Accordingly, “twenty per cent of $\text{HIS24}^+\text{TdT}^-\mu^-$ cells express Ig other than μ chains, with size distribution and kinetics similar to $\text{HIS24}^+\text{TdT}^-\text{Ig}^-$ cells” (Deenen *et al.*, 1987), and they are subtracted from this compartment. Similarly, six per cent of TdT^+ cells express μ chains, and were categorized as “pre-B cells”, and this portion is also subtracted from the TdT cell pool.

Table 5.3: Summary of flows between compartments and number of mitoses-for
Rat

FLOWS BETWEEN COMPARTMENTS ($\times 10^6$ cells/whole body BM/day)	HIS24		TdT		Pre-B		B		Total
	Small	Large	Small	Large	Small	Large	Small	Large	
Inflow from previous comp.	47.28		94.24		364.79		154.64		—
Inflow proliferation	262.01		65.63		448.43		n/a		776.07
Outflow to the next comp.	94.23		159.87		154.64		unknown		—
Outflow to the 2 nd next comp.	204.92		0.00		0.00		n/a		—
Outflow apoptosis	10.14		0.00		658.58		unknown		668.72
Sum of inflows	309.29		159.87		813.22		154.64		—
Sum of outflows	309.29		159.87		813.22		154.64		—
Balance (should be zero)	0.00		0.00		0.00		0.00		—
MITOSES									
Number of mitoses	2.71		0.76		1.16		n/a		4.63

As can be seen from the table, pre-B cells are the major precursor pool for the immature B cells, and pre-B cells are fed by both HIS24 cells and TdT cells. It was seen that even if the entire cell output of TdT pool is taken by the pre-B cell pool, it is not enough to replenish the pre-B cell compartment. Therefore it is seen that there is a mandatory positive flow from HIS24 cells to pre-B cells. This indicates that the unflow assumption would not yield feasible results for the rat B cell lineage, and that the TdT is NOT an obligatory stage in rat B cell genesis, and can be bypassed by a majority of cells that reside in HIS24 compartment. From the table it can be seen that outflows from the HIS24 compartment sum up to 309.29×10^6 cells, and 94.23×10^6 of that (which corresponds to 30% of the total flow) feeds the TdT cells, and 204.92×10^6 of it (66%) directly flows into the pre-B cell compartment. The rest of 3% is lost by apoptosis.

The major portion of cells that are lost to apoptosis are lost at the pre-B cell stage. From the total outflow (=inflow) of 813.22×10^6 cells, 658.58×10^6 of it are lost due to apoptosis, and only 154.64×10^6 of this amount can survive and feed the immature B cell pool. The apoptosis rate here corresponds to 80% of the total flow in the pre-B cell pool, which likely occurs at the small pre-B, immature B cell junction, as hypothesized by Deenen *et al.*, 1990.

HIS24⁺ and TdT⁺ precursors together produce about 780 million new cells per day in rat (as opposed to 80 million cells in mouse). Since we did not have any estimates for apoptosis for rat, we could not provide an estimate for the amount of outflow to the periphery, but even if there is no cell loss at the B cell stage, the maximum outflow would be around 150 million cells per day, which suggests that many more B cell precursors are produced than needed by the peripheral B cell pool, as in the case of mice.

The number of mitotic cycles is calculated in the same way as done previously, and it is found that on the average 4-5 mitoses occur in the rat B cell genesis. Our estimates of the number of mitoses for the HIS24⁺, TdT⁺ and pre-B cells are 2.71, 0.76, and 1.16, respectively.

We found that TdT is not an obligatory step, but can it be completely skipped by all of the precursor B cells in the lineage? To answer this question, we considered this possibility as well: that the TdT cells may not belong to the B cell lineage in rat BM, as mentioned as a possibility in Deenen *et. al*, 1987. The results are listed in Table 5.4, and our analysis revealed that this would not be possible due to the negative balance in HIS24 cell compartment (See the last row). These results suggest that TdT is not an obligatory step, and may be bypassed, but not exclusively. Put in other words, for every HIS24 cell, there is a chance of 66% to bypass the TdT stage, and directly feed the pre-B cell compartment.

Table 5.4: Summary of flows -without TdT

FLows BETWEEN COMPARTMENTS (×10⁶ cells/femur/hour)	HIS24	Pre-B	B
Inflow from previous compartment	47.28	364.79	154.54
Inflow proliferation	262.01	448.43	n/a
Outflow to the next compartment	364.79	154.64	unknown
Outflow apoptosis	0.00	658.58	unknown
Sum of inflows	309.29	813.22	154.54
Sum of outflows	364.79	813.22	154.54
Balance (should be zero)	-55.50	0.00	0.00

6. ANALYSIS OF THE MODEL

In this chapter, we will present the results of two different manipulations done at the initial model: 1- A change in the size of the late pro-B cells to test the relevancy of defining a Late Pro-B cell compartment, and 2-Adding a “reflux” from immature B cell to small pro-B cell compartment to simulate a condition which is called “receptor editing”.

6.1. Relevancy of the Late Pro-B cells

In our scheme, B220⁺μ⁻ cells appear as “late pro-B cells”, which are known to be functionally heterogeneous. Some of them are known to lack another B lineage marker not used in our scheme, the CD19. Therefore the late pro-B cell stage may include cells of natural killer or myeloid potential, as well as precursor B lineage cells. However, the existence of a late pro-B cell phenotype is demonstrated by relevant experiments (D.G. Osmond, unpublished).

Here we will also try to answer the question of to what extent late pro-B cells represent “either a stage in B-cell development intermediate between downregulation of TdT and detectable μ-chain synthesis or, alternatively, a population of preapoptotic cells with non-productive μ-chain gene rearrangements, earmarked for negative selection”, as mentioned as a possibility in Lu and Osmond, 2000.

We simulated this possibility by changing the number of cells per femur for the late pro-B cells from its normal size of 7×10^5 to a predefined percentage of it by changing it to $=7 \times (100 - \text{percent_late_pro}) / 100 \times 10^5$. The variable “percent_late_pro” is set to different values between 0-100, and it is seen that for all of its different values we still have a feasible data set (positive flows for the steady state and positive mitotic cycles). Three different values of the “percent_late_pro” and the resulted change in

flows are tabulated below in Tables 6.1-6.6 (which corresponds to 25%, 50% and 100% reduction in late pro-B cell compartment).

Table 6.1: Steady state flows when late pro-B cells are reduced by 25%

	Pro-B cells			Pre-B cells		B cells	Total
FLOWES BETWEEN COMPARTMENTS ($\times 10^4$ cells/femur/hour)	Early	Int.	Late	Large	Small	Immature	—
Inflow from previous compartment	1.24	1.49	2.05	4.52	8.72	4.64	—
Inflow proliferation	0.61	1.26	7.72	9.18	0.00	0.00	18.77
Outflow to the next compartment	1.49	2.05	4.52	8.72	4.64	0.46	—
Outflow apoptosis	0.36	0.70	5.25	4.98	4.08	4.18	19.55
Sum of inflows	1.85	2.75	9.77	13.70	8.72	4.64	—
Sum of outflows	1.85	2.75	9.77	13.70	8.72	4.64	—
Balance (should be zero)	0.00	0.00	0.00	0.00	0.00	0.00	—
MITOSES							
Number of mitoses	0.58	0.88	2.25	1.60	n/a	n/a	5.31

Table 6.2: Time constants when late pro-B cells are reduced by 25%

	Pro-B cells			Pre-B cells
TIME CONSTANTS	Early	Int.	Late	Large
cell cycle time calculated	13.90	7.72	5.16	4.30
experimental cell cycle time	19.60	13.50	7.40	6.50
avg transit time (calculated)	8.04	6.82	11.62	6.88
avg transit time (experimental)	11.34	11.92	16.66	10.40

Table 6.3: Steady state flows when late pro-B cells are reduced by 50%

	Pro-B cells			Pre-B cells		B cells	Total
FLOWES BETWEEN COMPARTMENTS ($\times 10^4$ cells/femur/hour)	Early	Int.	Late	Large	Small	Immature	—
Inflow from previous compartment	1.85	2.11	2.67	4.52	8.72	4.64	—
Inflow proliferation	0.61	1.26	5.36	9.18	0.00	0.00	16.41
Outflow to the next compartment	2.11	2.67	4.52	8.72	4.64	0.46	—
Outflow apoptosis	0.36	0.70	3.50	4.98	4.08	4.18	17.80
Sum of inflows	2.47	3.37	8.02	13.70	8.72	4.64	—
Sum of outflows	2.47	3.37	8.02	13.70	8.72	4.64	—
Balance (should be zero)	0.00	0.00	0.00	0.00	0.00	0.00	—
MITOSES							
Number of mitoses	0.41	0.68	1.59	1.60	n/a	n/a	4.28

Table 6.4: Time constants when late pro-B cells are reduced by 50%

	Pro-B cells			Pre-B cells
TIME CONSTANTS	Early	Int.	Late	Large
cell cycle time calculated	13.85	7.76	4.87	4.30
experimental cell cycle time	19.60	13.50	7.40	6.50
avg transit time (calculated)	5.70	5.25	7.74	6.88
avg transit time (experimental)	8.07	9.14	11.76	10.40

Table 6.5: Steady state flows when late pro-B cells are reduced by 100%

	Pro-B cells			Pre-B cells		B cells	Total
FLOWES BETWEEN COMPARTMENTS ($\times 10^4$ cells/femur/hour)	Early	Int.	Late	Large	Small	Immature	—
Inflow from previous compartment	3.08	3.33	3.89	4.52	8.72	4.64	—
Inflow proliferation	0.61	1.26	0.63	9.18	0.00	0.00	11.68
Outflow to the next compartment	3.33	3.89	4.52	8.72	4.64	0.46	—
Outflow apoptosis	0.36	0.70	0.00	4.98	4.08	4.18	14.30
Sum of inflows	3.69	4.59	4.52	13.70	8.72	4.64	—
Sum of outflows	3.69	4.59	4.52	13.70	8.72	4.64	—
Balance (should be zero)	0.00	0.00	0.00	0.00	0.00	0.00	—
MITOSES							
Number of mitoses	0.26	0.46	0.22	1.60	n/a	n/a	2.54

Table 6.6: Time constants when late pro-B cells are reduced by 100%

	Pro-B cells			Pre-B cells
TIME CONSTANTS	Early	Int.	Late	Large
cell cycle time calculated	13.77	7.77	0.00	4.30
experimental cell cycle time	19.60	13.50	7.40	6.50
avg transit time (calculated)	3.60	3.60	0.00	6.88
avg transit time (experimental)	5.13	6.25	1.60	10.40

It is observed that as the reduction in the percentage of late pro B cells increases, the number of mitotic cycles in each proliferating compartment decreases. The total number of mitotic cycles decreases from an average of 6.86 to 5.31 as the late pro B cells are decreased by 25%, and it further decreases to 4.28 and 2.54 as it becomes 50% and 0% of its normal value. Since it is believed that there is at least one mitotic cycle in each proliferating compartment, the average number of expected mitotic cycles in the B cell lineage seems to be greater or at least equal to 4, and a reduction of 100% does not seem very realistic. However it cannot also be denied that some portion of the late pro-B cells may not belong to a B cell, it seems very plausible that up to 30 % of the late pro-B cells may belong to other cell lineages. If we compare the

calculated cell cycle times it is again seen that the calculated values come closer to the experimental values as the percentage of reduction gets smaller, except for the intermediate pro-B cells.

6.2. Reflux due to Receptor Editing

We also simulated the hypothesis of a “reflux” from the immature B cell pool to the small pre-B cells due to receptor editing. We added another flow to the current structure, which represents the number of cells flowing from B to small pre-B cell pool per unit time (hours) (See Figure 6.1). The reflux constant is defined as the percentage of the B cells that flow back to the small pre-B cell compartment, and the resulting changes in steady state parameters are given in Table 6.7.

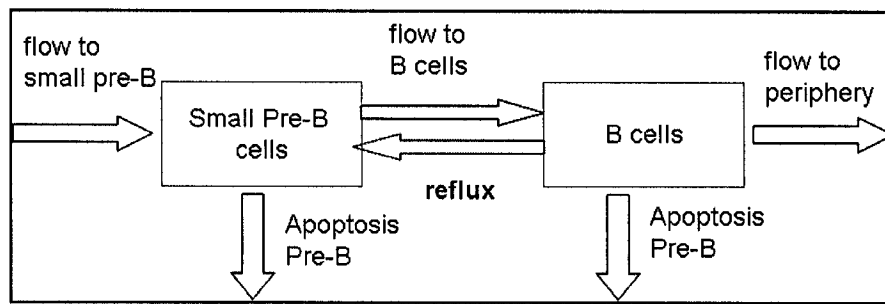


Figure 6.1: Testing the hypothesis of “reflux” from immature B cell to small pre-B cell pool- Change in model structure

Table 6.7: Steady state flows after imposing a “reflux” of 0.2% from immature B cell to small pre-B cell pool

	Pro-B cells			Pre-B cells		B cells	Total
	Early	Int.	Late	Large	Small	Immature	
FLOWES BETWEEN COMPARTMENTS ($\times 10^4$ cells/femur/hour)							
Inflow from previous compartment	0.63	0.88	1.44	4.52	8.72	4.64	—
Inflow proliferation	0.61	1.26	10.08	9.18	0.00	0.00	21.13
Outflow to the next compartment	0.88	1.44	4.52	8.72	4.64	0.00	—
Outflow apoptosis	0.36	0.70	7.00	4.98	4.54	4.18	21.76
Reflux	n/a	n/a	n/a	n/a	0.46	0.46	
Sum of inflows	1.24	2.14	11.52	13.70	9.18	4.64	—
Sum of outflows	1.24	2.14	11.52	13.70	9.18	4.64	—
Balance (should be zero)	0.00	0.00	0.00	0.00	0.00	0.00	—
MITOSES							

It is seen that positive values cannot be retained even after imposing a 5% reflux, and positive values are restricted to very small values for the reflux constant, e.g. 0.1% or up to a maximum of 0.2%. For the maximum value of 0.2, the reflux constitutes 10% of the total flow of the B cell compartment, and 5% of the total flow for the small pre-B compartment. It can be seen that there is no change in the estimates for the number of mitotic cycles, but the estimate for the apoptosis of the small pre-B cells has increased. From this experiment it can be concluded that a feasible data set can be found related to a hypothetical "reflux", but it constitutes only up to 10% of the flow between the compartments.

7. CONCLUSION AND FUTURE WORK

Mathematical models of physiological systems can make a significant contribution to the clinical diagnosis and to teaching of many aspects of physiology. They can also provide a means for evaluating hypotheses concerning the underlying pathology of a critical clinical disorder. This view has culminated in the growth of mathematical/simulation models that are employed as a tool for the understanding of physiological control systems, as well as the homeostatic regulation of haemopoetical cell lineages and their precursors in the bone marrow or in the periphery (Mackey and Dörmer, 1980, Mackey, 2001, Santillan *et al.*, 2000, Haurie *et al.*, 1998)

In this study, we aimed to develop and analyze a model for the proliferation and differentiation of mammalian B lymphocytes in laboratory mice and rats. To reach this goal, we first made an extensive summary of all the existing data on the various B cell precursors (for mice and rats) and organized it into a comprehensible framework. Then these data sets are used to build a mathematical model and to find all the crucial parameters to explain the existing steady state data e.g. the calculated flow from ‘compartment’ to ‘compartment’, the number of mitoses, and number of cells per clone). Then the model is used to test some of the hypotheses mentioned in the literature, i.e. relevancy of the late pro-B cells, and reflux due to receptor editing.

The steady state parameter estimates for mice and rat reveal that the number of cells lost due to apoptosis is about the same magnitude as the number of cells produced in the BM. Both the apoptotic rates and the production rates are also much higher than the number of cells necessary to replenish the peripheral B cell pool. This means that many more cells are produced (and then lost) than needed, which may be attributed to a great extent of a quality check in the B cell lineage, and a potential for the high variety of B cell repertoire. The stage at which apoptosis is triggered appears to vary between species. Whereas most of the cells are lost at the transition of small pre-B to B lymphocytes in rat BM, most of the loss in mice BM occurs before the small pre-B cell stage.

Another difference lies in the scheme of the lineages. In mice, the uniflow assumption of the Osmond group appears to give consistent results, whereas in rat, the TdT stage may be bypassed by some 30% of the cells, which suggests that it is not an obligatory step in rat BM. However it can also not be removed completely from the lineage, which suggests that the precursor-product relationship is less clear in rats than in mice, and the pre-B cells may be fed directly by all of its precursor cells. In mice, the late pro-B cell stage seems to be the most heterogeneous cell compartment, and experiments with the model parameters reveal that its real size can be less than its experimental value. Even a complete removal of this phenotypically defined compartment yields feasible results, however the calculated values get closer to the experimental values if the late pro-B compartment is included.

Both of the data sets we used for rat and mice are collected based on similar techniques and classification criteria, which made it possible to make a good comparison of the mathematically derived steady state parameter values for these two species. Once the framework for the mathematical model is established, the same analysis can be done for any precursor lymphocyte data set which is based on similar experimental techniques and classifications (e.g. measuring the rate of entry into mitosis, the turnover rate, etc.). The current framework does not include any homeostatic mechanisms, and the default assumption of the framework is the “unidirectional flow” between compartments. With some minor changes, homeostatic mechanisms and additional flows can be added to simulate and predict the responses of the system under investigation. However, it is necessary to have adequate experimental data to validate the simulation results; and it is usually not easy to find such data for the marrow lymphocytes.

As future work, the model that we developed here can be used to predict the temporal response to various experimental perturbations that have been reported from the laboratory of Prof. D. Osmond. A homeostatic feedback model can be employed, similar to previous mathematical T cell models, in which some of the rates are defined as a nonlinear relationship of population size, and a predefined “carrying capacity”.

The conclusions of a homeostatic model would have some implications for both of the normal regulation of B lymphopoiesis and of the dysregulated states leading to B-cell deficiencies and tumorigenesis. A good example of a disease condition is the dysregulation of the pre-B cell development associated with human cyclic neutropenia, which results in periodic excess numbers of pre-B cells in the BM. Homeostatic models are useful tools for analyzing important cyclicity-related parameters, e.g. the amplitude, period, and phase of oscillations.

GLOSSARY

Apoptotic index: Incidence of apoptotic cells

Apoptotic rate: Accumulation of apoptotic cells during short-term culture

Apoptotic transit time: The brief period between onset of apoptosis and clearance by macrophages

B220 (Tyrosine phosphatase B220): CD45RA isoform which is widely used as a B-lineage associated molecule

CFSE (CarboxyFluorescein diacetate Succinimidyl Ester): A cell division marker that acts as an intracellular fluorescent label for lymphocytes and dilutes after cell division

Femur: The long bone of the thigh, and the longest and strongest bone in the human body

Immunofluorescence: A technique that uses antibodies linked to a fluorescent dye in order to study antigens in a sample of tissue

In situ: In the natural or original position, “in situ DNA strand break labeling”

Ligation: The state of being bound “ligation by anti-IgM antibody”

Metaphase: Mitosis

Murine: Of or relating to common household rats and mice

Myelogenous: Originating in, or produced by the bone marrow, “myelogenous sarcoma”

Null lymphocytes: Newly formed small lymphocytes before the expression of surface IgM

TdT (Terminal deoxynucleotidyl transferase): An intranuclear enzyme restricted to immature lymphoid cells in the thymic cortex and BM

Tritiated: containing and especially labeled with tritium, “*in vivo* tritiated thymidine”

Vincristine sulfate: A metaphase blocking drug

REFERENCES

- Afonso R.M. Almeida a, Benedita Rocha b, Antonio A. Freitas a, Corine Tanchot, 2005, "Homeostasis of T cell numbers: from thymus production to peripheral compartmentalization and the indexation of regulatory T cells", *Seminars in Immunology*, Vol: 17, pp. 239-249.
- Agnes, F., M. M. Rosado and A. A. Freitas, "Independent homeostatic regulation of B cell compartments", *European Journal of Immunology*, Vol: 27, pp. 1801-1807.
- Allman, D. M., S. Ferguson, V. M. Lentz and M. Cancro, 1993, "Peripheral B cell maturation", *The Journal of Immunology*, Vol: 151, pp. 4431-4444.
- Bernard, S., L. Pujo-Menjouet and M. C. Mackey, 2003, "Analysis of Cell Kinetics Using a Cell Division Marker: Mathematical Modeling of Experimental Data", *Biophysical Journal*, Vol: 84, pp. 3414-3424.
- Bonhoeffer, S., H. Mohri, D. Ho and A. Perelson, 2000, "Quantification of cell turnover kinetics using 5-Bromo-2-deoxyuridine", *The Journal of Immunology*, Vol: 164, pp. 5049-5054.
- DeBoer, R. J., V. V. Ganusov, D. Milutinovic, P. D. Hodgkin and A. Perelson, 2006, "Estimating lymphocyte division and death rates from CFSE data", *Bulletin of Mathematical Biology*, Vol: 68, pp. 1011-31.
- DeBoer, R.J., A.A. Freitas and A. Perelson, "Resource Competition Determines Selection of B Cell Repertoires", *Journal of Theoretical Biology*, Vol: 212, pp. 333-343.
- Deenen, G. J., I. Van Balen and D. Opstelten, 1990, "In rat lymphocyte genesis sixty percent is lost from the BM at the transition of nondividing pre-B cell to sIgM⁺ B lymphocyte, the stage of Ig light chain gene expression ", *Eur. J. Immunology*, Vol. 20, pp. 557-564.
- Deenen, G. J., D. Opstelten, Rozing and Hunt, 1986, "B lymphocyte associated antigens on terminal Deoxynucleotidyl transferase- positive cells and pre-B cells in the rat", *The Journal of Immunology*, Vol: 137, pp. 76-84.
- Deenen, G. J., S. V. Hunt and D. Opstelten, 1987, "A stathmokinetic study of B lymphocytopoiesis in rat bone marrow: Proliferation of cells containing cytoplasmic μ -chains, TdT and carrying HIS24 antigen", *The Journal of Immunology*, Vol: 139, pp. 702-710.
- Deslauriers, Noëlla, 1982, "B cell differentiation and maturation in the BM: heterogeneity of B-cell precursors assessed by the appearance of age-related markers in functionally defined populations", *PhD Thesis*, Department of Medicine, McGill University.
- Deslauriers, Noëlla, 1982, "The nylon wool adherence marker of the B cell lineage appears at the resting pre-B cell stage", *European Journal of Immunology*, Vol: 12, pp. 285-289.

- Deslauriers-Boisvert, Noëlla, 1980, "Size separation and polyclonal activation to Ig secretion of early precursors of B lymphocytes", *The Journal of Immunology*, Vol: 125, pp. 47-52.
- Deslauriers, Noëlla, 1982, "Pre-B cell differentiation in the BM: a proliferative pathway parallels the post-mitotic maturation of early B cells", *European Journal of Immunology*, Vol: 12, pp. 922-926.
- Di Rosa, F., S. Ramaswamy, J. P. Ridge, P. Matzinger, 1999, "On the lifespan of virgin T lymphocytes", *The Journal of Immunology*, Vol: 163, pp. 1253-1257.
- Förster, I., 2004, "Analysis of B-Cell Life-Span and Homeostasis", *Methods in Molecular Biology*, Vol: 271, pp. 59-66.
- Förster, I. and K. Rajewski, 1990, "The bulk of the peripheral B-cell pool in mice is stable and not rapidly renewed from the bone marrow", *Immunology*, Vol: 87, pp. 4781-4784.
- Freitas, A. A., B. Rocha and A. A. Coutinho, 1986, "Lymphocyte population kinetics in the mouse", *Immunological Reviews*, Vol: 91, pp. 5-37.
- Freitas, A.A., B. Rocha, L. Forni and A. Coutinho, 1982, "Population dynamics of B lymphocytes and their precursors: demonstration of high turnover in the central and peripheral lymphoid organs", *J Immunol.*, Vol: 128, pp. 54-60.
- Fulop, G., J. Gordon and D. Osmond, 1983, "Regulation of lymphocyte production in the bone marrow", *The Journal of Immunology*, Vol: 130, pp. 644-648.
- Ganusov, V. V., R. Antia, R. Ahmed, R. de Boer, K. M. Krishna, S. S. Pilyugin, 2004, "Quantifying the immune cell turnover: Existing approaches to the same problem", MBI, Workshop 5.
- Gray, D., 1988, "Population kinetics of rat peripheral B cells", *Journal of Experimental Medicine*, Vol: 167, pp. 805-816.
- Hao, Z. and K. Rajewsky, 2001, "Homeostasis of Peripheral B Cells in the Absence of B Cell Influx from the Bone Marrow", *J. Exp. Med.*, Vol: 194, pp. 1151-1163.
- Haurie, C., D. C. Dale and M. C. Mackey, 1998, "Cyclical Neutropenia and Other Periodic Hematological Disorders: A Review of Mechanisms & Math. Models", *Blood*, Vol: 92, pp. 2629-2640.
- Hermans, M. H., H. Hartsuiker and D. Opstelten, 1989, "An In Situ Study of B lymphocytopoiesis in rat BM", *The Journal of Immunology*, Vol: 142, pp. 67-73.
- Johnson, K. M., Owen, K., P. L. Witte, 2002, "Aging and developmental transitions in the B cell lineage", *International Immunology*, Vol: 14, pp. 1313-1323.
- Landreth, K. S., C. Rosse and J. Clagett, 1981, "Myelogenous production and maturation of B lymphocytes in the Mouse", *The Journal of Immunology*, Vol: 127, pp. 2027-2034.
- Landreth, K. S. and P. W. Winkade, 1984, "Mammalian B lymphocyte precursors", *Developmental and Comparative Immunology*, Vol: 8, 773-790.
- Loder, F., B. Mutschler, R. J. Ray, C. J. Paige, P. Sideras, R. Torres, M. C. Lamers and R. Carsetti, 1999, "B cell development in the spleen takes place in discrete steps

and is determined by the quality of B cell receptor-derived signals", *Journal of Experimental Medicine*, Vol: 190, pp. 75-89.

- Lu, L. and D.G. Osmond, 1997, "Apoptosis during B lymphopoiesis in mouse bone marrow", *The Journal of Immunology*, Vol: 158, pp. 5136-5145.
- Lu, L., D. Lejtenyi and D.G. Osmond, 1999, "Regulation of cell survival during B lymphopoiesis: suppressed apoptosis of pro-B cells in P53-deficient mouse bone marrow", *European Journal of Immunology*, Vol: 29, pp. 2484-2490.
- Lu, L. and D. G. Osmond, 2000, "Apoptosis and its modulation during B lymphopoiesis in mouse bone marrow", *Immunological Reviews*, Vol: 175, pp. 158-174.
- Lu, L. and D.G. Osmond, 2001, "Regulation of cell survival during B lymphopoiesis in mouse bone marrow: Enhanced pre-B cell apoptosis in CSF-1 deficient op/op mutant mice", *Experimental Hematology*, Vol: 29, pp. 596-601.
- Lu, L., M. S. Chappel, R. K. Humphries and D.G. Osmond, 2000, "Regulation of cell survival during B lymphopoiesis: Increased pre-B cell apoptosis in CD-24-transgenic mouse bone marrow", *European Journal of Immunology*, Vol: 30, pp. 2686-2691.
- Lu, L., P. Chaudhury and D.G. Osmond, 1999, Regulation of cell survival during B lymphopoiesis: Apoptosis and Bcl-2/Bax content of precursor B cells in BM of mice with altered expression of IL7 and recombinaise activating gene, *The Journal of Immunology*, Vol: 162, pp. 1931-1940.
- Lu, L., G. Smithson, P. W. Kincade and D. G. Osmond, 1998, "Two models of murine B lymphopoiesis: a correlation", *European Journal of Immunology*, Vol: 28, pp. 1755-1761.
- Macallan, D. C., D. L. Wallace, Y. Zhang, H. Ghattas, B. Asquith, C. Lara, A. Worth, G. Panayiotakopoulos, G. E. Griffin, D. F. Tough and P. C. L. Beverley, 2005, "B-cell kinetics in humans: rapid turnover of peripheral blood memory cells", *Immunobology*, Vol: 105, pp. 3633-3640.
- Mackey, M. C., 2000, "Cell kinetic status of haemotopoietic stem cells", *Cell Proliferation*, Vol: 34, pp 71-83.
- Mackey, M.C., A.A. Aprikyan and D.C. Dale, 2003, "The rate of apoptosis in post mitotic neutrophil precursors of normal and neutropenic humans", *Cell Proliferation*, Vol: 36, pp. 27-34.
- Mackey, M. C. and P. Dörmer, 1982, "Continuous maturation of proliferating erythroid precursors", *Cell Tissue Kinetics*, Vol: 15, pp. 381-392.
- Mackey, M. C. and P. Dörmer, 1981, "Enigmatic Hemapoiesis", *Biomathematics and Cell Kinetics*, pp. 87-103.
- McLean, A.R., M.M. Rosado, F. Agenes, R. Vasconcellos and A. A. Freitas, 1997, "Resource competition as a mechanism for B cell homeostasis", *Immunology*, Vol: 94, pp. 5792-5797.
- MacLennan, Ian C. M. and D. Gray, 1986, "Antigen-driven selection of virgin and memory B cells", *Immunological Reviews*, Vol: 91, pp. 61-81.
- MacLennan, I. and E. Chan, 1993, "The dynamic relationship between B-cell populations in adults", *Immunology Today*, Vol: 14, pp. 29-34.

- Mehr, R., A. Perelson, M. Fridkis-Hareli and A. Globerson, 1996, "Feedback regulation of T cell development in the thymus", *Journal of Theoretical Biology*, Vol: 181, pp. 157-167.
- Mehr, R., A. Perelson, M. Fridkis-Hareli and A. Globerson, 1997, "Regulatory feedback pathways in the thymus", *Immunology Today*, Vol: 18, pp. 581-585.
- Mehr, R., A. Globerson and A. Perelson, 1995, "Modeling Positive and Negative Selection and Differentiation Processes in the Thymus", *Journal of Theoretical Biology*, Vol: 175, pp. 103-126.
- Mehr, M., L. Abel, P. Ubezio, A. Globerson and Z. Agur, 1993, "A mathematical model of the effect of aging on bone marrow cells colonizing the thymus", *Mechanisms of Ageing and Development*, Vol: 67, pp. 159-172.
- Mehr, R., G. Shahaf, A. Sah and M. Cancro, 2003, "Asynchronous differentiation models explain BM labeling kinetics and predict reflux btw the pre-and immature B cell pools", *International Immunology*, Vol: 15, pp. 301-312.
- Metcalf, D., 1963, "The autonomous behavior of normal thymus grafts", *The Australian Journal of Experimental Biology and Medical Science*, Vol: 41, pp. 437-448.
- Miller, S. C and D. G. Osmond, 1973, "The proliferation of lymphoid cells in guinea-pig bone marrow", *Cell Tissue Kinetics*, Vol: 6, pp. 259-269.
- Miller, S. C., Y. Yoshida and D. G. Osmond, 1973, "Kinetic and haemopoietic properties of lymphoid cells in the bone marrow", *Reprinted from Haemopoietic Stem Cells*, Vol: pp. 131-155.
- Miller, S. C. and D. G. Osmond, 1975, "Lymphocyte populations in mouse bone marrow: Quantitative kinetic studies in young, pubertal and adult C3H mice", *Cell Tissue Kinetics*, Vol: 8, pp. 97-110.
- Nossal G. J. and D. G. Osmond, 1974, "Differentiation of lymphocytes in mouse bone marrow", *Cellular Immunology*, Vol: 13, pp. 132-145.
- Novak, J.P. and E. Necas, 1994, "Proliferation-differentiation pathways of murine haemopoiesis: correlation of lineage fluxes", *Cell Prolif.*, Vol: 27, pp. 597-633
- Opstelten, D., G. J. Deenen, J. Rozing and S.V. Hunt, 1985, "Pre-B cells in Rat Bone Marrow: Identification, surface markers and isolation", *Adv. Exp. Med. Biol.*, Vol: 186, pp. 9-16.
- Opstelten, D., G. J. Deenen, J. Rozing and S. Hunt, "B lymphocyte associated antigens on terminal Deoxynucleotidyl transferase-positive cells and pre-B cells in bone marrow of the rat", *The Journal of Immunology*, Vol: 137, pp. 76-84.
- Osmond, D. G., 1990, "B cell development in the bone marrow", *Seminars in Immunology*, Vol: 2, pp.173-180.
- Osmond, D. G., A. Rolink and F. Melchers, 1998, "Murine B lymphopoiesis: towards a unified model", *Immunology Today*, Vol: 19, pp. 65-68.
- Osmond, D.G., S.Rico-Vargas, H. Valenzona, L. Fauteux, L. Liu, R. Janani, L. Lu and K. Jacobsen, 1994, "Apoptosis and macrophage-mediated cell deletion in the regulation of B lymphopoiesis in mouse bone marrow", *Immunological Reviews*, Vol: 142, pp. 209-230.

- Osmond, D. G., N. Kim, R. Manoukian, R. A. Phillips, S. A. Rico-Vargas and K. Jacobsen, 1992, "Dynamics and Localization of Early B-Lymphocyte Precursor Cells (Pro-B Cells) in the Bone Marrow of scid Mice", *Blood*, Vol: 79, pp. 1695-1703.
- Opstelten, D. and D. G. Osmond, 1985, "Regulation of pre-B cell proliferation in bone marrow: immunofluorescence stathmokinetic studies of cytoplasmic μ chain-bearing cells", *European Journal of Immunology*, Vol: 15, pp. 599-605.
- Opstelten, D. and D. G. Osmond, 1983, "Pre-B cells in mouse bone marrow: Immunofluorescence stathmokinetic studies of the proliferation", *The Journal of Immunology*, Vol: 131, pp. 2635-2639.
- Osmond, D. G., 1993, "The turnover of B-cell populations", *Immunology Today*, Vol: 14, pp. 34-37.
- Park, Y. H. and D.G. Osmond, 1988, "Post irradiation regeneration of early B-lymphocyte precursor cells in mouse bone marrow", *Immunology*, Vol: 66, pp. 343-347.
- Park, Y. H. and D. G. Osmond, 1987, "B lymphocyte progenitors in mouse bone marrow", *International Review of Immunology*, Vol: 2, pp. 241-261.
- Park, Y. H. and D. G. Osmond, 1989, "Dynamics of early B lymphocyte precursor cells in mouse bone marrow: proliferation of cells containing terminal deoxynucleotidyl transferase", *European Journal of Immunology*, Vol: 19, pp. 2139-2144.
- Rajewsky, K., 1993, "B-cell lifespans in the mouse why to debate what?", *Immunology Today*, Vol: 14, pp. 469-470.
- Rocha B, C. Penit, C. Baron, F. Vasseur, N. Dautigny and A. A. Freitas, 1990, "Accumulation of bromodeoxyuridine-labeled cells in central and peripheral lymphoid organs: minimal estimates of production and turnover rates of mature lymphocytes", *Eur J Immunol*, Vol: 20, pp. 1697-1708.
- Röpke, C. and N. B. Everett, 1975, "Life span of small lymphocytes in the thymolymphatic tissues of normal and thymus-deprived BALB/C mice", *Anat. Rec*, Vol: 183, pp. 83-94.
- Rubinow, S. I. and J. L. Lebowitz, 1975, "A mathematical model of neutrophil production and control in normal man", *Journal of Mathematical Biology*, Vol: 1, pp. 187-225.
- Shahaf, G. D. Allman, M. P. Cancro and R. Mehr, 2004, "Screening of alternative models for transitional B cell maturation", *International Immunology*, Vol: 16, pp. 1081-1090.
- Sprent, J. and D. F. Tough, 1994, "Lymphocyte life-span and memory", *Science*, Vol: 265, pp. 1395-1400.
- Srivastava, B., R. C. Lindsley, N. Nikbakht and D. Allman, "Models for peripheral B cell development and homeostasis", *Seminars in Immunology*, Vol: 17, pp. 175-182.
- Su, T. T. and D. Rawlings, 2002, "Transitional B lymphocyte subsets operate as distinct checkpoints in murine splenic B cell development", *The Journal of Immunology*, Vol: 168, pp. 2101-2110.

- Tanchot, C. and B. Rocha, 1998, "The organization of mature T-cell pools", *Immunology Today*, Vol: 19, pp. 575-579.
- Tanchot, C., M. M. Rosado, F. Agenes, A. A. Freitas and B. Rocha, 1997, "Lymphocyte homeostasis", *Seminars in Immunology*, Vol: 9, pp. 331-337.
- U.T.M.D. Anderson Cancer Centre Science Park - Research Division website:
http://sciencepark.mdanderson.org/fcores/flow/files/DNA_PI.html
- Valenzona, H. O., R. Pointer, R. Ceredig and D. G. Osmond, 1996, "Prelymphomatous B cell hyperplasia in the bone marrow of interleukin-7 transgenic mice", *Experimental Hematology*, Vol: 24, pp. 1521-1529.
- Yu, Q., P. Laneuville and D.G. Osmond, 2001, "Suppressed apoptosis of pre-B cells in bone marrow of pre-leukemic p190^{bcr/abl} transgenic mice", *Leukemia*, Vol: 15, pp. 819-827.
- Yu, Q., S.C. Miller and D.G. Osmond, 2000, "Melatonin inhibits apoptosis during early B-cell development in mouse bone marrow", *Journal of Pineal Research*, Vol: 29, pp. 86-93.